The Business Cycle Mechanics of Search and Matching Models*

Joshua Bernstein

Alexander W. Richter   Nathaniel A. Throckmorton

August 31, 2020

ABSTRACT

This paper provides new insights into the business cycle mechanics of search and matching models. We develop a novel identification scheme based on the matching elasticity that allows these models to perfectly match a range of labor market moments. Our estimated linear model also matches several non-targeted moments including the Beveridge curve and the decomposition of inflows and outflows of unemployment. A structural decomposition reveals job separation rate shocks explain 40% of unemployment volatility. The nonlinear version of our model generates state-dependent dynamics that produce empirically consistent fluctuations in output growth uncertainty, 37% of which stem from separation rate shocks.

Keywords: Labor Market Flows; Job Separation Rate; Business Cycles; Estimation; Nonlinear
JEL Classifications: C13; E24; E32; E37; J63

*Bernstein, Department of Economics, Indiana University, 100 S. Woodlawn, Bloomington, IN 47405 (jmbernst@iu.edu); Richter, Research Department, Federal Reserve Bank of Dallas, 2200 N Pearl Street, Dallas, TX 75201 (alex.richter@dal.frb.org); Throckmorton, Department of Economics, William & Mary, P.O. Box 8795, Williamsburg, VA 23187 (nat@wm.edu). This work was supported by computational resources provided by the BigTex High Performance Computing Group at the Federal Reserve Bank of Dallas. The views expressed in this paper are our own and do not necessarily reflect the views of the Federal Reserve Bank of Dallas or the Federal Reserve System.

1 INTRODUCTION

Short-run fluctuations in unemployment are a key component of modern business cycles. Developing quantitative frameworks that can account for these fluctuations remains an active area of research. Even in a model without investment or risk aversion, Shimer (2005) shows labor market volatility is low under common parameterizations. In response to this puzzle, recent work has used simple frameworks to shed light on mechanisms that generate empirically consistent labor market fluctuations (Hagedorn and Manovskii, 2008; Hall and Milgrom, 2008; Ljungqvist and Sargent, 2017; Pissarides, 2009). Using these observations as a point of departure, we provide new qualitative and quantitative insights into the business cycle mechanics of search and matching models.

We conduct our analysis using a real business cycle model with unemployment à la Diamond-Mortensen-Pissarides. The model is driven by estimated stochastic processes for labor productivity and the job separation rate. The paper makes three contributions to the literature. First, we develop an identification scheme that allows the model to exactly match a range of labor market moments, including the volatilities of unemployment and vacancies. Our identification scheme shows how model parameters are connected to the data in ways calibration exercises may obscure. For example, we show how the elasticity of matches with respect to unemployment determines the volatility of vacancies relative to the volatility of unemployment. Intuitively, when the matching elasticity is higher, a given increase in matches requires a smaller increase in unemployment. Therefore, as matches fluctuate over the business cycle, unemployment fluctuates less relative to vacancies.

To generate realistic volatilities of both unemployment and vacancies, we combine the matching elasticity with the "fundamental surplus," defined as the marginal product of labor minus any resources that are not allocated to vacancy creation (Ljungqvist and Sargent, 2017). The fundamental surplus sets the level of labor market volatility, while the matching elasticity determines how the volatility is split between vacancies and unemployment. To demonstrate the advantage of our approach, we contrast our results with a model in which the matching elasticity is implied by targeting average labor market tightness (e.g., Hagedorn and Manovskii, 2008). In this case, the model produces substantial labor market volatility, but the split between unemployment and vacancies is far from the data. The implied matching elasticity is also outside of the plausible range (Mortensen and Nagypal, 2007; Petrongolo and Pissarides, 2001), in sharp contrast with our estimated model.

The model simultaneously matches the volatilities of aggregate consumption, investment, unemployment, and vacancies. In addition to matching these targeted moments, our estimated model closely matches a range of non-targeted moments, validating the model's propagation mechanisms. Importantly, the correlation of unemployment with vacancies (i.e., the Beveridge curve) is consistent with the data. The model also produces realistic volatilities of the job finding rate and the net exit rate, which measures the net flow into unemployment within a period. In addition, the model generates endogenous persistence beyond the exogenous driving processes, which is crucial for the model to match the persistences of unemployment, vacancies, the job finding rate, and net exit rate.

Our second contribution uses our model to revisit the transmission of shocks to the job separation rate. We begin by offering a structural interpretation of an open empirical question: how much unemployment volatility is explained by variation in the job separation rate? Shimer (2012) finds job separation rate shocks account for at most 25% of the variation in unemployment in the data. However, as Barnichon (2012) points out, this result is based on the assumption that the job finding and job separation rates are independent. After relaxing this assumption, the empirical contribution of job separation rate shocks rises to 40%. We implement two decompositions and show that our model is consistent with both of these findings. First, we estimate the reduced-form regression of Shimer (2012), and find that separation rate shocks account for 25%-30% of unemployment variation. Second, we use our model to construct a fully structural decomposition that controls for the dependence of the job finding rate on job separation rate shocks. We find job separation rate shocks account for 30% of variation in the job finding rate. Once we account for this, the contribution of job separation rate shocks to unemployment volatility naturally increases. In the baseline log-linear version of our model, variation in the job separation rate on average accounts for 50% of unemployment volatility. The contribution falls to 40% when we solve the model nonlinearly to account for state-dependence in the underlying shocks, which is in line with Barnichon (2012).

We then turn to the transmission of job separation rate shocks, distinguishing between shocks that affect only the job separation rate and shocks that also affect labor productivity according to the strength of their empirical correlation. Accounting for this correlation is crucial. In the absence of an associated decline in labor productivity, an increase in job separations causes unemployment and vacancies to increase, which contrasts with the negatively sloped Beveridge curve observed in the data. Allowing for a correlated decline in labor productivity in our model prevents this counterfactual outcome and strengthens the macroeconomic responses to a job separation rate shock.

We also find meaningful state-dependence in the impulse responses when we solve our model nonlinearly. For example, unemployment rises about 50% more in response to a job separation rate shock when the economy is already in a recession where the unemployment rate is 10%. This endogenous amplification complements the results for labor productivity shocks analyzed by Petrosky-Nadeau et al. (2018) and provides an additional source of endogenous disaster dynamics.

Finally, we show the nonlinearities in our model generate endogenous uncertainty—the expected volatility of the one-month ahead forecast error of output growth. Although we do not target uncertainty moments, the volatility of uncertainty in our model is close to reduced-form empirical measures (Jurado et al., 2015) and consistent with the empirical finding that uncertainty about real activity is typically an endogenous response to business cycles rather than an exogenous propagation (Ludvigson et al., 2020). When we decompose uncertainty into its structural components, job separation rate shocks explain 37% of its variation. These results show that job separation rate shocks also have an important role in explaining variation in higher-order moments.

Related Literature The literature on search and matching in a business cycle setting is extensive. Our analysis stays close to the quantitative tradition of the early literature (Andolfatto, 1996; Den Haan et al., 2000; Merz, 1995), while building on the insights of the recent literature that abstracts from capital and curvature in utility (Hagedorn and Manovskii, 2008; Ljungqvist and Sargent, 2017; Mortensen and Nagypal, 2007; Shimer, 2005). Relative to these influential papers, we develop a complete and portable parameter identification scheme that improves on the standard calibration approach. We emphasize how the matching elasticity drives relative labor market volatility and validate our estimation strategy using a range of goods and labor market moments.

We highlight the importance of exogenous variation in the job separation rate in explaining business cycle fluctuations. This emphasis contrasts with much of the literature that either abstracts from variation in the job separation rate altogether or treats it as purely endogenous (Den Haan et al., 2000; Fujita and Ramey, 2012). The tight link between job separations and productivity in these papers results in a much stronger negative correlation than what we measure in the data. To attain a realistic correlation, we assume variation in the job separation rate is exogenous and estimate its correlation with labor productivity by targeting this moment in the data. Our approach is similar to Coles and Kelishomi (2018), who study how separation rate shocks and vacancy adjustment frictions interact in a search and matching model. The estimated model matches job separation rate moments in the data, including their reduced-form contribution to unemployment volatility (Barnichon, 2012; Elsby et al., 2009; Shimer, 2012). This framework also allows us to study the transmission of separation rate shocks, which is impossible in a purely endogenous setup.

Our estimation-based approach is related to recent work by Christiano et al. (2016), who estimate a New Keynesian model with labor market frictions to match identified impulse responses of macroeconomic variables to monetary and technology shocks. Relative to their analysis, we offer a complementary approach to the identification of key model parameters. Furthermore, we pay special attention to the role of job separation rate shocks, including their state-dependent effects.

To our knowledge, we are the first to analyze endogenous uncertainty in a search and matching model. Our results are consistent with the growing empirical literature that measures macro uncertainty and its effects in the data (Jurado et al., 2015; Ludvigson et al., 2020). From a theoretical perspective, our analysis offers a new mechanism for generating time-varying endogenous uncertainty that complements papers focused on financial (Brunnermeier and Sannikov, 2014; Mendoza, 2010; Plante et al., 2018), firm default (Arellano et al., 2019), or incomplete information channels (Fajgelbaum et al., 2017; Straub and Ulbricht, 2015; Van Nieuwerburgh and Veldkamp, 2006).

The paper proceeds as follows. Section 2 introduces our model, while Section 3 details our data and estimation strategy. Section 4 presents our quantitative results, and Section 5 concludes.

2 MODEL

We situate our analysis in a real business cycle model, augmented to include a frictional labor market similar to Merz (1995) and Andolfatto (1996). Relative to Shimer (2005), these frameworks include capital and curvature in utility. Time is discrete and the population is normalized to unity.

Aggregate Shocks There are two sources of aggregate fluctuations: shocks to labor productivity $\varepsilon_{a,t}$ and the job separation rate $\varepsilon_{s,t}$. The shocks are independent standard normal random variables.

Search and Matching At the beginning of period t, the employment rate is n_{t-1}. A fraction s_t of employed workers are then separated from their jobs. The exogenous job separation rate follows

$$\ln s_{t+1} = (1-\rho_s)\ln \bar{s} + \rho_s \ln s_t + \rho_{as}\sigma_a\varepsilon_{a,t+1} + \sigma_s\varepsilon_{s,t+1}, \tag{1}$$

where ρ_{as} determines the cross-correlation between the job separation rate and labor productivity.

We assume newly separated workers are able to search for new jobs within the same period as their job loss. However, it is natural that these workers will have less time to search for new jobs than those who became unemployed in a previous period. Therefore, let $\chi \in [0,1]$ denote the fraction of a period that newly unemployed workers spend searching for work within the same period as their job loss. Then the number of unemployed people searching for work is given by

$$u_t^s = u_{t-1} + \chi s_t n_{t-1}. \tag{2}$$

Shimer (2005) makes this point when constructing a measure of the monthly job finding rate in the data. To deal with this "time aggregation bias", he sets $\chi = 0.5$, while we estimate the value of χ.

Following Den Haan et al. (2000), if a firm posts v_t vacancies the number of matches is given by

$$m_t = u_t^s v_t/((u_t^s)^\iota + (v_t)^\iota)^{1/\iota}, \tag{3}$$

where $\iota > 0$ controls the elasticity of matches with respect to unemployed searching. Define $\theta_t \equiv v_t/u_t^s$ as labor market tightness. Then the job finding rate f_t and job filling rate q_t are given by

$$f_t = m_t/u_t^s = 1/(1+\theta_t^{-\iota})^{1/\iota}, \tag{4}$$

$$q_t = m_t/v_t = 1/(1+\theta_t^{\iota})^{1/\iota}. \tag{5}$$

Following Blanchard and Galí (2010), we assume newly matched workers begin employment in the same period they are matched with a firm, so aggregate employment evolves according to

$$n_t = (1-s_t)n_{t-1} + m_t. \tag{6}$$

The unemployment rate, u_t, includes anyone who is not employed in period t, so it satisfies

$$u_t \equiv u_t^s - m_t = 1 - n_t. \tag{7}$$

Households Following Merz (1995) and Andolfatto (1996), employed and unemployed workers pool their incomes in a representative family. A family head chooses optimal paths for consumption and capital investment, taking the paths for aggregate employment and unemployment as given. Investment is subject to capital adjustment costs, so the capital stock evolves according to

$$k_t = (1-\delta)k_{t-1} + \left(a_1 + \frac{a_2}{1-1/\nu}\left(\frac{i_t}{k_{t-1}}\right)^{1-1/\nu}\right)k_{t-1}, \tag{8}$$

where $0 < \delta < 1$ is the capital depreciation rate, $\nu > 0$ determines the size of the capital adjustment cost, and $a_1 = \delta/(1-\nu)$ and $a_2 = \delta^{1/\nu}$ are chosen so there are no adjustment costs in steady state.

The representative family solves

$$J_t^H = \max_{c_t, i_t, k_t} \ln c_t + \beta E_t[J_{t+1}^H] \tag{9}$$

subject to (8) and

$$c_t + i_t = w_t n_t + r_t^k k_{t-1} + d_t, \tag{10}$$

$$n_{t+1} = (1 - s_{t+1}(1 - \chi f_{t+1}))n_t + f_{t+1}u_t, \tag{11}$$

$$u_{t+1} = s_{t+1}(1 - \chi f_{t+1})n_t + (1 - f_{t+1})u_t, \tag{12}$$

where w_t is the wage, r_t^k is the rental return on capital, d_t is firm dividends, and E_t is the mathematical expectation operator conditional on information at time t. The optimality conditions imply

$$\frac{1}{a_2}\left(\frac{i_t}{k_{t-1}}\right)^{1/\nu} = E_t\left[x_{t+1}\left(r_{t+1}^k + \frac{1}{a_2}\left(\frac{i_{t+1}}{k_t}\right)^{1/\nu}(1-\delta+a_1) + \frac{1}{\nu-1}\frac{i_{t+1}}{k_t}\right)\right], \tag{13}$$

where $x_t = \beta(c_{t-1}/c_t)$ is the household's stochastic discount factor. Condition (13) says the marginal cost of investing in period t is equal to the marginal benefit in period $t+1$, which includes the return on capital, the undepreciated capital stock, and the foregone capital adjustment cost.

Firms A representative firm produces output with a Cobb-Douglas production function given by

$$y_t = k_{t-1}^{\alpha}(a_t n_t)^{1-\alpha}, \tag{14}$$

where $0 < \alpha < 1$ is the income share of capital, and labor productivity a_t evolves according to

$$\ln a_{t+1} = (1-\rho_a)\ln \bar{a} + \rho_a \ln a_t + \rho_{as}\sigma_s\varepsilon_{s,t+1} + \sigma_a\varepsilon_{a,t+1}. \tag{15}$$

To hire workers, the firm posts vacancies v_t that are subject to a per unit cost κ. In addition, the firm rents capital from the household at rental rate r_t^k and pays its workers a wage w_t determined by a Nash bargaining process described below. Therefore, the firm maximizes profits by solving

$$J_t^F = \max_{k_{t-1},n_t,v_t} y_t - w_t n_t - r_t^k k_{t-1} - \kappa v_t + E_t[x_{t+1} J_{t+1}^F] \tag{16}$$

subject to (14) and

$$n_t = (1 - s_t)n_{t-1} + q_t v_t, \tag{17}$$

$$v_t \geq 0. \tag{18}$$

Letting $\lambda_{n,t}$ denote the Lagrange multiplier on (17), the optimality conditions are given by

$$r_t^k = \alpha y_t / k_{t-1}, \tag{19}$$

$$\lambda_{n,t} = (1 - \alpha) y_t / n_t - w_t + E_t[x_{t+1}(1 - s_{t+1})\lambda_{n,t+1}], \tag{20}$$

$$q_t \lambda_{n,t} = \kappa - \lambda_{0,t}. \tag{21}$$

The first condition (19) sets the marginal product of capital equal to its rental rate, while (20) recursively defines the marginal benefit of hiring an additional worker. Finally, (21) states that the firm's optimal vacancy creation choice sets the expected marginal benefit of a vacancy $q_t \lambda_{n,t}$ equal to its marginal cost: the costs of creating the vacancy today minus the savings from relaxing the non-negativity constraint. Also note that $\lambda_{n,t}$ is the marginal surplus of a new match to the firm.

Wages As noted by Hall (2005), there are many ways to determine wages in search and matching models. To facilitate comparison, we follow the bulk of the literature and assume wages are determined via Nash bargaining between an employed worker and the firm. To operationalize this wage protocol, we define the total surplus of a match as $\Lambda_t = \lambda_{n,t} + W_t - U_t$, where W_t and U_t satisfy

$$W_t = w_t + E_t[x_{t+1}((1 - s_{t+1}(1 - \chi f_{t+1}))W_{t+1} + s_{t+1}(1 - \chi f_{t+1})U_{t+1})]$$

$$U_t = b + E_t[x_{t+1}(f_{t+1} W_{t+1} + (1 - f_{t+1})U_{t+1})].$$

W_t is the capitalized value of employment for the worker, while U_t and b define the worker's highest credible payoff from walking away from the wage negotiation (i.e., the worker's outside option).

We are deliberately agnostic about the sources of the worker's outside option b. In reality, it could consist of many components from both the worker's and firm's microeconomic environments. For example, the worker may receive unemployment benefits or attain a utility payoff from leisure time. Alternatively, if the firm faces fixed costs of hiring such as training costs or layoff taxes (Petrosky-Nadeau et al., 2018; Pissarides, 2009), then the worker may be able to bargain over how much of these costs are reflected in equilibrium wages, effectively improving her threat point.[1]

We ultimately estimate b to match the volatilities of unemployment and vacancies in the data. Following Ljungqvist and Sargent (2017), what matters for this estimation is the size of b relative to the marginal product of labor. The decomposition of b into its underlying components is irrelevant. In addition, it is misleading to only model a subset of the possible components of b. For example, in a model in which b reflects mainly the value of the leisure component, Chodorow-Reich and Karabarbounis (2016) show the resulting pro-cyclicality of the worker's outside option dampens labor market volatility even if its average level is high. Therefore, there must be another component of b that is strongly countercyclical to offset the dampening effect. We make b an estimated parameter, since it is beyond the scope of this paper to decipher its exact microeconomic components.[2]

The equilibrium wage rate maximizes $(W_t - U_t)^\eta \lambda_{n,t}^{1-\eta}$, where $\eta \in [0,1]$ is the household's bargaining weight. The optimality condition implies $W_t - U_t = \eta\Lambda_t$ or, equivalently, $\lambda_{n,t} = (1-\eta)\Lambda_t$. To derive the equilibrium wage, plug (20) in for $\lambda_{n,t}$ and combine the two conditions to obtain

$$w_t = \eta((1-\alpha)y_t/n_t + E_t[x_{t+1}(1-\chi s_{t+1})f_{t+1}\lambda_{n,t+1}]) + (1-\eta)b. \tag{22}$$

The wage rate in period t is a weighted average of the firm's value of a new match and the worker's outside option b. The firm's value of a new worker includes the additional output produced plus the discounted expected value of the foregone vacancy cost net of separations that occur in period $t+1$.

Equilibrium The aggregate resource constraint is given by

$$c_t + i_t + \kappa v_t = y_t. \tag{23}$$

A competitive equilibrium includes sequences of quantities $\{c_t, i_t, n_t, k_t, y_t, u_t, u_t^s, v_t, q_t, \lambda_{0,t}\}_{t=0}^\infty$, prices $\{w_t, r_t^k\}_{t=0}^\infty$, and exogenous variables $\{a_t, s_t\}_{t=1}^\infty$ that satisfy (1), (2), (5)-(8), (13)-(15), (19)-(21), (22), and (23), given the initial conditions $\{k_{-1}, n_{-1}, a_{-1}, s_{-1}\}$ and shocks $\{\varepsilon_{a,t}, \varepsilon_{s,t}\}_{t=0}^\infty$.

3 DATA AND ESTIMATION PROCEDURE

This section begins by describing our data and the empirical targets in our estimation. It then outlines our new identification scheme and provides a detailed account of our estimation methodology.

3.1 EMPIRICAL TARGETS

The model is disciplined using a balanced sample from 1955Q1-2019Q4. Appendix A provides a description of our data sources and how they were transformed.

[1]In the alternative-offer bargaining protocol of Hall and Milgrom (2008), the worker's bargaining position is stronger when firms incur higher costs from delaying the period in which the equilibrium wage is agreed upon.

[2]Mortensen and Nagypal (2007) combine multiple components of b to generate realistic labor market volatility. Costain and Reiter (2008) show that search and matching models struggle to simultaneously match labor market volatilities and the responses to changes in labor market policies such as unemployment insurance benefits. Resolving this issue is outside our identification strategy since we do not need to model how labor market policies may affect b.

Labor Market Moments The job finding rate, $f_t = 1 - (U_{t+1} - U^s_{t+1})/U_t$ is based on Shimer (2005), where U_t is total unemployed and U^s_t is the subset who are unemployed 1 month or less. Following Shimer (2012), the monthly job separation rate is $s_t \equiv 1 - \exp(-\tilde{s}_t)$, where $\tilde{s}_t$ satisfies

$$U_{t+1} = (1 - e^{-\tilde{f}_t - \tilde{s}_t})\tilde{s}_t LF_t/(\tilde{f}_t + \tilde{s}_t) + e^{-\tilde{f}_t - \tilde{s}_t}U_t,$$

LF_t is the labor force, and $\tilde{f}_t \equiv -\log(1 - f_t)$. The unemployment rate is $u_t = U_t/LF_t$. The vacancy rate v_t is based on the series in Barnichon (2010) until 2000, after which it is equal to job openings as a share of the labor force in the Job Openings and Labor Turnover Survey. These series correct for trends in the print and online help-wanted indexes published by the Conference Board. The rates are converted to a quarterly frequency by averaging across the months in each quarter.

Following Shimer (2005), labor productivity is output per job in the non-farm business sector, while the wage rate is the ratio of labor compensation to employment in the non-farm business sector. To remove time trends, we filter the data following Hamilton (2018) (henceforth, Hamilton) by regressing each variable on its most recent four lags after an 8 quarter window. We use this approach over the more common Hodrick and Prescott (1997) filter because Hodrick (2020) shows the Hamilton filter performs better when time series, such as these, are first difference stationary.

Using these time series, we compute the following estimation targets: the means of the quarterly unemployment, job finding, and job separation rates, the standard deviations of the unemployment and vacancy rates, the standard deviation and autocorrelation of the job separation rate, the standard deviation and autocorrelation of labor productivity, the cross-correlation between labor productivity and the job separation rate, and the elasticity of wages with respect to productivity (computed as the slope coefficient from regressing log wages on an intercept and log productivity).

Goods Market Moments In addition to the 11 labor market moments, we target the standard deviations and autocorrelations of consumption and investment growth. Consumption includes expenditures on services and nondurables. Investment is composed of durable consumption and private fixed investment. The growth rates are computed as quarter-over-quarter log differences.

3.2 IDENTIFICATION Before estimating the model, we first describe the mapping between the model parameters and moments that are measurable in the data. We estimate 12 model parameters: $b, \iota, \eta, \kappa, \chi, \bar{s}, \rho_s, \sigma_s, \rho_a, \sigma_a, \sigma_{a,s}, \nu$. While these parameters are jointly estimated, we can heuristically describe how each parameter is identified from specific moments that we compute in the data.

Table 1 summarizes the identification scheme. The outside option b governs the economy's "fundamental surplus fraction" (Ljungqvist and Sargent, 2017), defined as the upper bound on the fraction of a worker's output that can be allocated to vacancy creation. It is now well understood that a small fundamental surplus fraction is crucial to deliver realistically large volatilities of unemployment and vacancies (Hagedorn and Manovskii, 2008; Ljungqvist and Sargent, 2017). To

Parameters	Identifying Moments
b, ι	$SD(u), SD(v)$
η	$Cov(w, a)/Var(a)$
κ, χ	$E(u), E(f)$
$\bar{s}, \rho_s, \sigma_s, \rho_a, \sigma_a, \sigma_{a,s}$	$E(s), AC(s), SD(s), AC(a), SD(a), Corr(a, s)$
ν	$SD(c), SD(i), AC(c), AC(i)$

Table 1: Identification heuristic. E, SD, Var, AC, $Corr$, Cov denote the mean, standard deviation, variance, autocorrelation, cross-correlation, and covariance over our balanced sample from 1955Q1-2019Q4.

see this, consider the steady-state vacancy creation condition in a model without capital ($\alpha = 0$),

$$\frac{\kappa}{\bar{q}} = \frac{(1-\eta)(\bar{a}-b)}{1-\beta(1-\bar{s})+\eta\beta(1-\chi\bar{s})\bar{f}}, \tag{24}$$

where bars denote steady states. The elasticity of tightness with respect to productivity is given by,

$$\bar{\epsilon}_{\theta,a} = \frac{\bar{a}}{\bar{a}-b} \times \frac{1-\beta(1-\bar{s})+\eta\beta(1-\chi\bar{s})\bar{f}}{\bar{\epsilon}_{m,u^s}(1-\beta(1-\bar{s}))+\eta\beta(1-\chi\bar{s})\bar{f}}, \tag{25}$$

where $(\bar{a} - b)/\bar{a}$ is the fundamental surplus fraction and $\bar{\epsilon}_{m,u^s}$ is the steady-state elasticity of matches with respect to the mass of unemployed searching. The second term in this expression is near unity since $\beta(1 - \bar{s}) \approx 1$ at a monthly frequency. Therefore, to generate a large response of tightness (and hence unemployment and vacancies) to changes in productivity, the fundamental surplus fraction must be small, which requires that b is close to the marginal product of labor $\bar{a}$. A small fundamental surplus fraction makes the fundamental surplus very sensitive to changes in productivity, which causes volatile changes in the resources allocated to vacancy creation. Hence, we estimate b by targeting the standard deviations of unemployment and vacancies in the data.

While b affects the overall level of labor market volatility, we now show that ι affects the relative volatilities of vacancies and unemployment. First note that our matching function specification implies that $\bar{\epsilon}_{m,u^s} = \bar{f}^{\iota}$, where $\bar{f}$ is the steady-state job finding rate. Therefore, given an average job finding rate (that we target using other parameters), ι pins down the elasticity of matches with respect to unemployed searching.[3] To see the role that $\bar{\epsilon}_{m,u^s}$ plays, we compute the elasticities of unemployment and vacancies with respect to tightness in the simplified model, which are given by[4]

$$\bar{\epsilon}_{u,\theta} = -(1-\bar{u})(1-\bar{\epsilon}_{m,u^s})/(1-\chi\bar{f}), \tag{26}$$

$$\bar{\epsilon}_{v,\theta} = 1-(1-\bar{u})(1-\bar{\epsilon}_{m,u^s})/(1-\chi\bar{f}). \tag{27}$$

As $\bar{\epsilon}_{m,u^s}$ increases, the responsiveness of vacancies to changes in tightness grows relative to the

[3]Our argument also applies to the Cobb-Douglas matching function $m_t = \mu(u_t^s)^\alpha v_t^{1-\alpha}$. In this case, $\bar{\epsilon}_{m,u^s} = \alpha$.
[4]These come from differentiating the steady-state conditions $\bar{u} = \bar{s}(1-\chi\bar{f})/(\bar{s}(1-\chi\bar{f})+\bar{f})$ and $\bar{v} = \bar{\theta}\bar{u}^s$.

responsiveness of unemployment. Intuitively, when the elasticity is higher, a given increase in matches requires a smaller increase in unemployed searching, and hence in unemployment. Therefore, when matches fluctuate, unemployment fluctuates less relative to vacancies. Hence, we estimate ι by targeting the *relative* standard deviations of unemployment and vacancies in the data.

Recall from (22) that η governs the responsiveness of wages to changes in the marginal product of labor, which is driven by labor productivity. Hence, we follow Hagedorn and Manovskii (2008) and estimate η by targeting the empirical elasticity of wages with respect to labor productivity.

The last two labor market parameters κ and χ are estimated by targeting the average unemployment rate and job finding rate. To see this mapping, consider the following steady-state conditions

$$\bar{f} = \bar{\theta}/(1+\bar{\theta}^{\iota})^{1/\iota}, \tag{28}$$

$$(\kappa/\bar{q})(1-\beta(1-\bar{s})+\eta\beta(1-\chi\bar{s})\bar{f}) = (1-\eta)(\bar{a}-b), \tag{29}$$

$$\bar{u} = \bar{s}(1-\chi\bar{f})/(\bar{s}(1-\chi\bar{f})+\bar{f}). \tag{30}$$

Given ι, targeting the average job finding rate identifies the average tightness $\bar{\theta}$ from (28), and hence $\bar{q} = \bar{f}/\bar{\theta}$. Combining with a target for average unemployment, we can then solve (29) and (30) for κ and χ, given all of the other parameters. The parameters governing the exogenous processes $\bar{s}, \rho_s, \sigma_s, \rho_a, \sigma_a, \rho_{a,s}$ have empirical counterparts in the data, so we estimate these parameters by directly targeting these moments. Finally, we estimate the capital adjustment cost parameter ν by targeting the standard deviations and autocorrelations of investment and consumption growth.

3.3 ESTIMATION PROCEDURE

First, we externally set three parameters in line with the business cycle literature. The time discount factor, β, is set to 0.9983, which implies an annual real interest rate of 2%. The capital depreciation rate, $\delta = 0.0077$, matches the annual average rate on private fixed assets and consumer durable goods converted to a monthly rate. The income share of capital, $\alpha = 0.3845$, equals the complement of the quarterly labor share in the non-farm business sector.

The 15 target moments are stored in $\hat{\Psi}_T^D$ and estimated using a two-step Generalized Method of Moments (GMM) estimator with a balanced sample of $T = 260$ quarters. Given the GMM estimates, we estimate our model with Simulated Method of Moments (SMM) to account for potential short-sample bias. For parameterization ϑ and shocks $\mathcal{E} = \{a, s\}$, we solve the log-linear model using Sims (2002) `gensys` algorithm and simulate it $R = 1{,}000$ times for T periods. The model analogues of the target moments are the median moments across the R simulations, $\bar{\Psi}_{R,T}^M(\theta, \mathcal{E})$.

The parameter estimates, $\hat{\vartheta}$, are obtained by minimizing the following loss function:

$$J(\vartheta, \mathcal{E}) = [\hat{\Psi}_T^D - \bar{\Psi}_{R,T}^M(\vartheta, \mathcal{E})]'[\hat{\Sigma}_T^D(1+1/R)]^{-1}[\hat{\Psi}_T^D - \bar{\Psi}_{R,T}^M(\vartheta, \mathcal{E})],$$

where $\hat{\Sigma}_T^D$ is the diagonal of the GMM estimate of the variance-covariance matrix. We use Monte

Carlo methods to calculate the standard errors on the parameter estimates. For different sequences of shocks, we re-estimate the structural model $N_h = 100$ times and report the mean and $(5, 95)$ percentiles of the parameter estimates.[5] Appendix B provides additional details on the methodology.

4 Quantitative Analysis

In this section, we first report the estimated parameters and demonstrate the quantitative fit of our model in both a linear and nonlinear setting. We then use the estimated model as a lens to study the transmission of job separation rate shocks and the propagation of endogenous uncertainty.

4.1 Parameter Estimates and Model Fit Table 2 reports the targeted empirical and simulated moments across a range of specifications. We begin by discussing the estimates from the log-linear version of our model. To gauge the success of our identification scheme for the labor market parameters, we first compare the data to the model when we only target labor market moments. As shown in the "Linear-Labor" column, the linear model is able to perfectly match the data for each targeted moment, indicating the strength of our proposed identification scheme.

The "Linear-Labor" column of Table 3 reports the corresponding estimated parameters. The mean estimates are well within conventional ranges and the standard errors are small. Relative to Hagedorn and Manovskii (2008), we estimate a considerably larger bargaining weight $\eta = 0.46$ (cf., $\eta = 0.052$). The higher estimate of η is due to the presence of capital in our model, which weakens the response of the marginal product of labor to changes in labor productivity. The estimate of κ implies that vacancy creation costs account for less than 1% of output on average. Relatedly, our estimate of $b = 0.96$ is consistent with these small costs and the small fundamental surplus Ljungqvist and Sargent (2017) show is required to generate realistic labor market volatility.

Our identification strategy yields an estimate for $\chi = 0.53$. This value is remarkably close to the assumption of $\chi = 0.5$ that Shimer (2005) makes when computing his empirical measure of the job separation rate series. Following his intuition, $\chi = 0.53$ implies newly separated workers have around two weeks on average to find another job before the next measurement of unemployment.[6]

Having established the success of our identification scheme, we now examine the first column of the "Labor & Goods" moments section of Table 2. In this specification, we estimate all parameters including ν using the full list of moments in Table 1. The first takeaway is that the model's performance in the labor market dimension remains strong when we also target the goods market moments. The t-statistics for the null hypothesis that a model-implied moment equals its empirical counterpart remain close to zero. The estimated model parameters are also essentially unchanged.

[5] Ruge-Murcia (2012) applies SMM to several nonlinear business cycle models and finds that asymptotic standard errors tend to overstate the variability of the estimates. This underscores the importance of using Monte Carlo methods.

[6] We compute our own series for the empirical job separation rate using the continuous time methodology in Shimer (2012). Therefore, our finding that χ is close to 0.5 is not simply a result of our construction of the separation rate.

		Labor	Labor & Goods		
Moment	Data	Linear	Linear	$\bar{\theta} = 0.634$	Nonlinear
$E(u)$	5.89	5.89 (0.00)	5.92 (0.13)	5.95 (0.24)	6.18 (1.26)
$E(f)$	42.14	42.14 (0.00)	42.02 (−0.11)	43.36 (1.08)	40.37 (−1.57)
$E(s)$	3.27	3.27 (0.00)	3.27 (−0.01)	3.27 (−0.01)	3.27 (−0.02)
$SD(u)$	22.25	22.25 (0.00)	22.70 (0.24)	30.97 (4.79)	23.04 (0.43)
$SD(v)$	22.99	22.99 (0.00)	22.95 (−0.02)	16.15 (−3.57)	22.92 (−0.04)
$SD(s)$	8.66	8.66 (0.00)	8.67 (0.01)	8.67 (0.01)	8.66 (0.00)
$SD(a)$	2.63	2.63 (0.00)	2.68 (0.27)	2.68 (0.27)	2.67 (0.25)
$SD(\Delta \log c)$	0.51	0.16* (−8.36)	0.50 (−0.22)	0.56 (1.10)	0.53 (0.32)
$SD(\Delta \log i)$	2.12	2.88* (4.22)	2.06 (−0.33)	2.23 (0.61)	2.13 (0.02)
$AC(s)$	0.79	0.79 (0.00)	0.79 (0.09)	0.79 (0.09)	0.79 (0.08)
$AC(a)$	0.90	0.90 (0.00)	0.91 (0.34)	0.91 (0.34)	0.91 (0.34)
$AC(\Delta \log c)$	0.29	0.45* (1.93)	0.23 (−0.76)	0.23 (−0.71)	0.24 (−0.65)
$AC(\Delta \log i)$	0.44	0.21* (−3.17)	0.21 (−3.10)	0.22 (−3.05)	0.22 (−2.95)
$Corr(s, a)$	−0.47	−0.47 (0.00)	−0.47 (−0.01)	−0.47 (−0.01)	−0.47 (0.03)
$Cov(w, a)/Var(a)$	0.47	0.47 (0.00)	0.45 (−0.30)	0.41 (−0.94)	0.43 (−0.60)
J		0.00	10.72	49.42	14.01

Table 2: Model fit for targeted moments. The t-statistic for the null hypothesis that a model-implied moment equals its empirical counterpart is shown in parentheses. The first column reports the GMM estimates of the empirical targets. The second column sets $\nu \to \infty$ and only targets the labor market moments (asterisks indicate non-targeted moments). The third column includes the goods market moments and estimates ν. The fourth column sets ι to target average labor market tightness, $\bar{\theta} = 0.634$, following Hagedorn and Manovskii (2008) and sets κ to retain the mean finding rate in the data. The final column reports moments from the nonlinear model using the parameter estimates from the linear model. All monthly time series are averaged to a quarterly frequency and the data is detrended using a Hamilton (2018) filter with an 8 quarter window.

Second, targeting good market moments and estimating ν improves the model's ability to match the volatilities and autocorrelations of consumption and investment growth.[7] When only targeting the labor market moments, the estimated model fails to reproduce the standard deviations and auto-

[7]Our model is deliberately parsimonious to highlight our main points related to the labor market. Other features such as home production, habits in preferences, and variable capital utilization could further improve the model's fit.

	Labor	Labor & Goods	
Parameter	Linear	Linear	$\bar{\theta} = 0.634$
$\bar{s}$	0.0325 (0.0325, 0.0326)	0.0325 (0.0325, 0.0326)	0.0325 (0.0325, 0.0326)
ρ_a	0.9533 (0.9524, 0.9542)	0.9577 (0.9569, 0.9586)	0.9577 (0.9569, 0.9586)
σ_a	0.0073 (0.0073, 0.0074)	0.0071 (0.0070, 0.0073)	0.0071 (0.0070, 0.0073)
ι	0.5955 (0.5908, 0.6007)	0.6046 (0.5966, 0.6117)	1.1419 (1.1419, 1.1419)
η	0.4621 (0.4445, 0.4836)	0.4784 (0.4155, 0.5543)	0.4784 (0.4155, 0.5543)
b	0.9599 (0.9596, 0.9603)	0.9622 (0.9617, 0.9626)	0.9622 (0.9617, 0.9626)
κ	0.0214 (0.0196, 0.0229)	0.0202 (0.0150, 0.0258)	0.0572 (0.0421, 0.0721)
χ	0.5334 (0.5278, 0.5388)	0.5336 (0.5274, 0.5406)	0.5336 (0.5274, 0.5406)
ρ_s	0.8940 (0.8927, 0.8952)	0.8960 (0.8937, 0.8982)	0.8960 (0.8937, 0.8982)
σ_s	0.0414 (0.0412, 0.0416)	0.0410 (0.0405, 0.0415)	0.0410 (0.0405, 0.0415)
ρ_{as}	−0.0999 (−0.1016, −0.0983)	−0.1002 (−0.1030, −0.0969)	−0.1002 (−0.1030, −0.0969)
ν	–	4.9665 (4.9196, 5.0122)	4.9665 (4.9196, 5.0122)

Table 3: Mean estimates of the model parameters. The $(5, 95)$ percentiles are shown in parentheses. Each column corresponds to a different estimation specification. The first column sets $\nu \to \infty$ and only targets the labor market moments. The second column includes the goods market moments and estimates ν. The final column sets ι to target average labor market tightness, $\bar{\theta} = 0.634$, following Hagedorn and Manovskii (2008) and sets κ to retain the mean finding rate in the data (the remaining parameters are not re-estimated).

correlations of consumption and investment growth in the data. In the fully estimated model, only the autocorrelation of investment growth remains significantly different from the data. Given this success, we conduct the rest of our analyses using the estimation that targets all 15 data moments.

Matching Function Identification We estimate the matching function curvature parameter ι so the model produces empirically consistent relative volatilities of unemployment and vacancies. This approach contrasts with the literature, which often calibrates ι to hit a steady-state target. To demonstrate the advantages of our approach, we compare our results to a model calibrated in the style of Hagedorn and Manovskii (2008). Holding other parameters fixed at their estimated values, we set ι to target an average tightness of $\bar{\theta} = 0.634$ and set κ to retain an average finding rate in the data. The "$\bar{\theta} = 0.634$" columns of Tables 2 and 3 show the estimated moments and parameters.

Under this calibration, labor market volatility remains substantially elevated as a result of the small fundamental surplus fraction. However, the relative volatilities of unemployment and vacancies are now far from the data. The model over-predicts unemployment volatility and under-predicts vacancy volatility. This discrepancy is explained by the matching elasticities implied by the baseline estimation ($\bar{\epsilon}_{m,u^s} = 0.59$) and alternate calibration ($\bar{\epsilon}_{m,u^s} = 0.37$). The lower elasticity implies that unemployment volatility must increase relative to vacancy volatility. As a result, the model is unable to match these key targets, even though it still performs well in other dimensions.[8] Furthermore, our estimate of $\bar{\epsilon}_{m,u^s}$ is in the middle of the plausible range of elasticities (0.5-0.7) highlighted by Mortensen and Nagypal (2007), while the alternate elasticity is far below the range.

Finally, we stress that our approach is *not* inconsistent with also targeting an average value for labor market tightness or, equivalently, long run values for the job finding and job filling rates. To achieve this, we could augment the matching function with an efficiency parameter μ so that $m_t = \mu u_t^s v_t/((u_t^s)^\iota + (v_t)^\iota)^{1/\iota}$. We could then estimate μ to target an average value for θ using the steady-state relationship $\bar{f} = \mu\bar{\theta}/(1+\bar{\theta}^\iota)^{1/\iota}$, while still using ι to attain a matching elasticity $\bar{\epsilon}_{m,u^s} = \bar{f}^\iota/\mu^\iota$ that implies the best fit of the unemployment and vacancy volatilities in the data.[9]

Non-targeted moments To further validate our estimated framework, we report a range of non-targeted moments. Table 4 shows several key labor market statistics. We report the results when only the labor market moments in Table 1 are targeted, but we focus on the case that targets all 15 moments. The model produces a range of non-targeted labor market moments that are close to their empirical counterparts. In particular, the model almost exactly matches the volatility of the job finding rate and closely matches the volatility of the net unemployment inflow rate $z_t = s_t(1-\chi f_t)$. In addition, the model generates realistic persistence in unemployment, vacancies, and the job finding and inflow rates, as indicated by their high autocorrelations, which are all close to the data.

These findings further emphasize the advantage of how we estimate ι. Comparing results to the alternate calibration that sets $\bar{\theta} = 0.634$, the job finding rate becomes far too volatile due to the excess volatility of unemployment, while vacancies are no longer persistent enough. The additional vacancy persistence in our baseline model is generated by the higher matching elasticity, which strengthens the propagation mechanism from the underlying persistent shocks. The baseline model also generates a realistic decomposition of the fluctuations of unemployment into inflows and outflows. Following Shimer (2012), we compute the share of unemployment volatility explained by outflows (i.e., the job finding rate) by regressing $\bar{s}/(\bar{s} + f_t)$ on the unemployment rate. This yields an outflow share of 69% in the model, which accords well with the 73% reported in the data.

We now turn to Table 5, which reports the correlations analyzed by Shimer (2005). The baseline model closely matches most of the cross-correlations in the data. For example, it matches the

[8] Hagedorn and Manovskii (2008) calibrate their model at a weekly frequency. Their calibration implies a matching elasticity of $\bar{\epsilon}_{m,u^s} = 0.45$ that results in counterfactually high vacancy volatility relative to unemployment volatility.

[9] Using a Cobb-Douglas matching function $m_t = \mu u_t^\alpha v_t^{1-\alpha}$, Shimer (2005) exploits the same feature to argue that average tightness is irrelevant since μ can always target it. We adopt his logic by normalizing μ to unity in our model.

		Labor	Labor & Goods		
Moment	Data	Linear	Linear	$\bar{\theta} = 0.634$	Nonlinear
$E(z)$	2.55	2.55 (-0.01)	2.55 (0.02)	2.54 (-0.08)	2.57 (0.24)
$SD(f)$	15.87	15.46 (-0.20)	15.81 (-0.03)	22.94 (3.41)	17.00 (0.54)
$SD(z)$	12.21	10.98 (-1.26)	11.08 (-1.16)	12.64 (0.44)	10.92 (-1.33)
$AC(f)$	0.90	0.93 (0.88)	0.93 (0.83)	0.93 (0.78)	0.92 (0.59)
$AC(u)$	0.92	0.93 (0.35)	0.93 (0.35)	0.94 (0.56)	0.94 (0.43)
$AC(v)$	0.93	0.87 (-2.09)	0.87 (-2.27)	0.75 (-6.15)	0.84 (-2.98)
$AC(z)$	0.87	0.82 (-1.37)	0.83 (-1.26)	0.84 (-0.77)	0.82 (-1.38)
$Cov(\frac{\bar{s}}{\bar{s}+f}, u)/Var(u)$	72.90	69.15 (-0.27)	69.15 (-0.27)	73.66 (0.06)	72.27 (-0.05)

Table 4: Model fit for non-targeted moments. The t-statistic for the null hypothesis that a model-implied moment equals its empirical counterpart is shown in parentheses. The first column reports the GMM estimates of the non-targeted data moments. The second column sets $\nu \to \infty$ and only targets the labor market moments in Table 1. The third column includes the goods market moments in Table 1 and estimates ν. The fourth column sets ι to target average labor market tightness, $\bar{\theta} = 0.634$, following Hagedorn and Manovskii (2008) and sets κ to retain the mean finding rate in the data. The final column reports moments from the nonlinear model using the parameter estimates from the linear model. All monthly time series are averaged to a quarterly frequency and the data is detrended using a Hamilton (2018) filter with an 8 quarter window.

Beveridge curve (i.e., the correlation between vacancies and unemployment). It is also successful at producing reasonable cross-correlations with vacancies, though the correlation with the job separation rate is quite small relative to the data.[10] Importantly, our identification scheme produces a closer fit of the data than the alternate calibration along these key dimensions. For example, targeting $\bar{\theta} = 0.634$ results in a much flatter Beveridge curve since unemployment fluctuates more than vacancies. Furthermore, vacancies become positively correlated with the job separation rate.

Nonlinearities Recent work by Petrosky-Nadeau and Zhang (2017) and Petrosky-Nadeau et al. (2018) shows that a calibrated version of the search and matching model with productivity shocks produces significant nonlinearities. Given their findings, we complement our results from the linear version of our model by studying how our estimated model behaves when it is solved nonlinearly.

We solve the nonlinear model with the policy function iteration algorithm described in Richter et al. (2014), which is based on the theoretical work on monotone operators in Coleman (1991). Using the linear solution as an initial conjecture, the algorithm minimizes the Euler equation errors

[10] Similar to Shimer (2005) and Hagedorn and Manovskii (2008), the baseline model overstates the correlation between unemployment and labor productivity in the data. However, as Barnichon (2012) shows, the empirical correlation switched sign from negative to positive in the 1980s, making it difficult to draw direct comparisons to the data.

		Labor	Labor & Goods		
Moment	Data	Linear	Linear	$\bar{\theta} = 0.634$	Nonlinear
$Corr(u, v)$	-0.77	-0.78 (-0.19)	-0.78 (-0.23)	-0.68 (1.88)	-0.77 (0.06)
$Corr(u, f)$	-0.85	-0.94 (-3.31)	-0.95 (-3.38)	-0.97 (-4.14)	-0.94 (-3.15)
$Corr(u, s)$	0.44	0.59 (1.69)	0.60 (1.72)	0.52 (0.94)	0.58 (1.54)
$Corr(u, a)$	-0.28	-0.90 (-5.66)	-0.92 (-5.85)	-0.92 (-5.84)	-0.91 (-5.73)
$Corr(v, f)$	0.82	0.94 (3.87)	0.94 (3.83)	0.84 (0.79)	0.93 (3.57)
$Corr(v, s)$	-0.39	-0.07 (3.59)	-0.08 (3.45)	0.05 (4.91)	-0.07 (3.59)
$Corr(v, a)$	0.12	0.82 (6.45)	0.84 (6.65)	0.73 (5.57)	0.82 (6.45)
$Corr(f, s)$	-0.25	-0.34 (-0.72)	-0.35 (-0.82)	-0.34 (-0.77)	-0.33 (-0.64)
$Corr(f, a)$	0.20	0.91 (6.09)	0.93 (6.29)	0.92 (6.17)	0.91 (6.09)

Table 5: Model fit for non-targeted correlations. The t-statistic for the null hypothesis that a model-implied moment equals its empirical counterpart is shown in parentheses. The first column reports the GMM estimates of the non-targeted data moments. The second column sets $\nu \to \infty$ and only targets the labor market moments in Table 1. The third column includes the goods market moments in Table 1 and estimates ν. The fourth column sets ι to target average labor market tightness, $\bar{\theta} = 0.634$, following Hagedorn and Manovskii (2008) and sets κ to retain the mean finding rate in the data. The final column reports moments from the nonlinear model using the parameter estimates from the linear model. All monthly time series are averaged to a quarterly frequency and the data is detrended using a Hamilton (2018) filter with an 8 quarter window.

on every node in the discretized state space. It then computes the maximum distance between the policy functions across all nodes and iterates until that distance falls below the tolerance criterion.

Two aspects of the solution method require special attention. First, we adapt the Rowenhorst method to discretize the correlated separation rate and labor productivity processes into two independent N-state Markov chains following Galindev and Lkhagvasuren (2010). Second, we follow Garcia and Zangwill (1981) and introduce an auxiliary variable that is continuous in the state of the economy to ensure that vacancies do not violate the non-negativity constraint. Appendix C provides detailed descriptions of these features as well as the policy function iteration algorithm.

The last columns in Tables 2, 4, and 5 show the targeted and non-targeted moments implied by the nonlinear model under the parameter estimates from the linear model when labor and goods moments are targeted. Without exception, the moments from the nonlinear model are very similar to the moments from the linear model. While the overall fit of the model would improve slightly if we re-estimated the parameters, these results indicate that there would be little change. Therefore, we will continue to use the linear parameter estimates when further analyzing the nonlinear model.

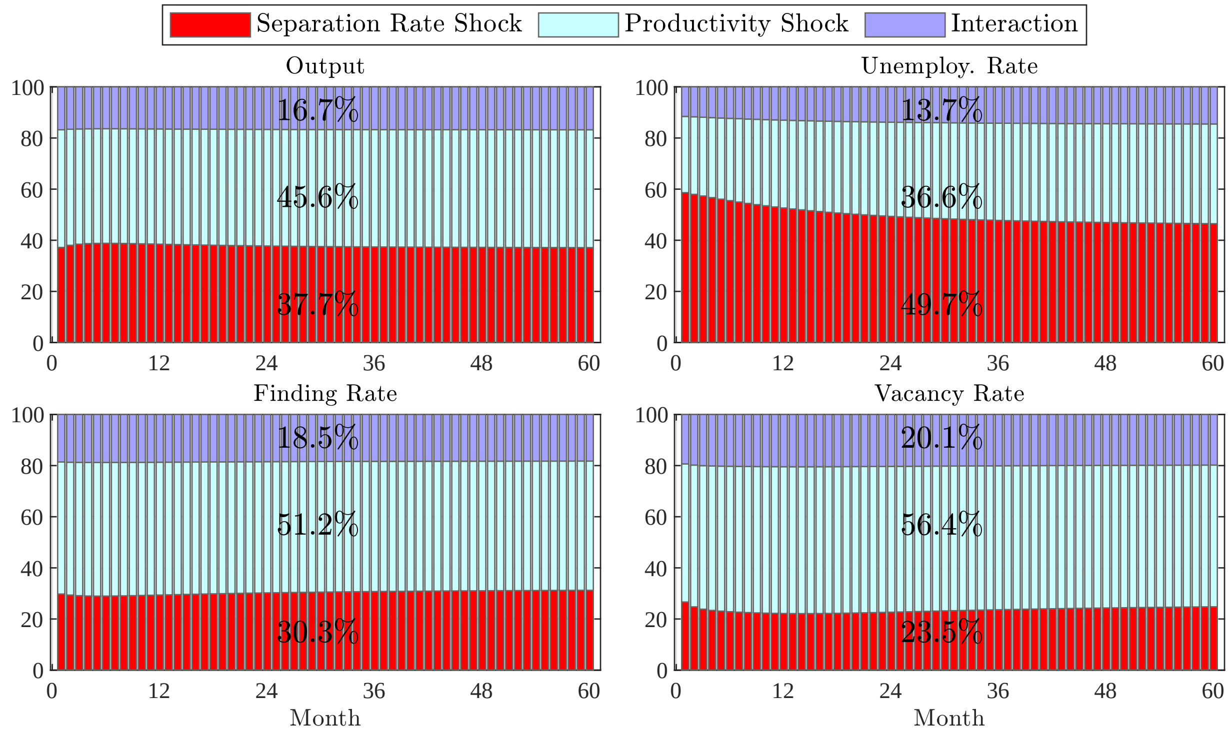

(a) Linear Model Forecast Error Variance Decomposition

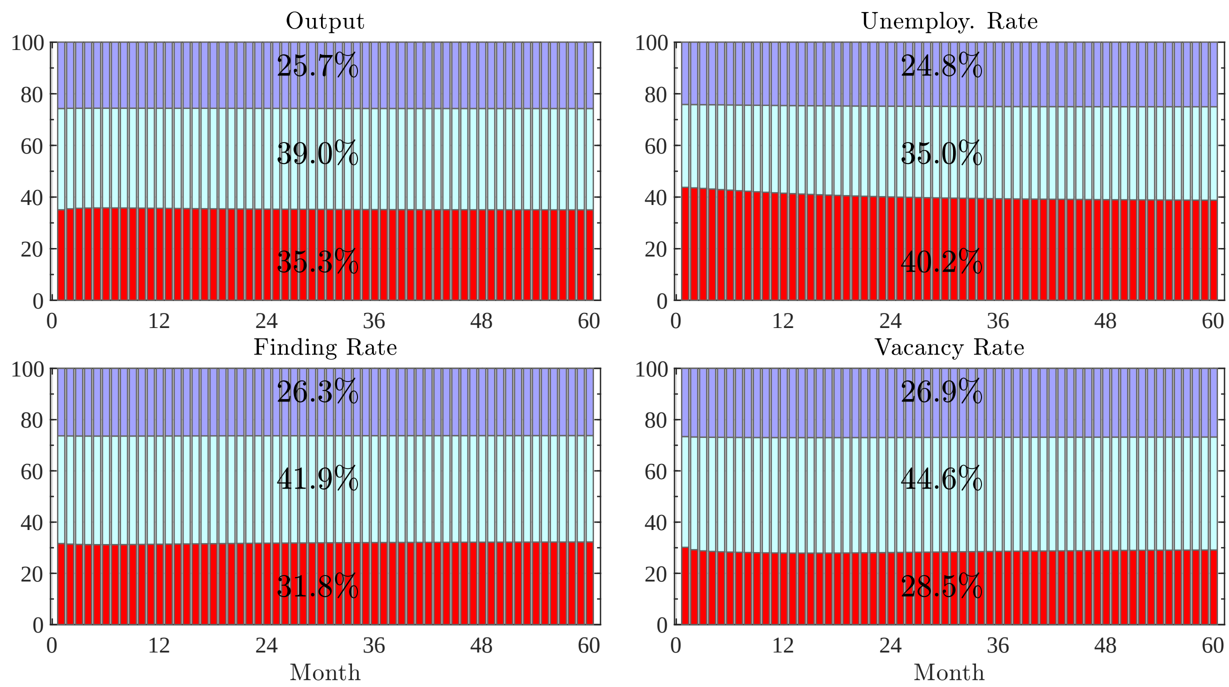

(b) Nonlinear Model Generalized Forecast Error Variance Decomposition

Figure 1: Forecast error variance decompositions. Each plot decomposes the forecast error variance into variation from job separation rate shocks, labor productivity shocks, and their interaction. Values are then normalized by the sum of the components, since the three contributions will not necessarily sum to unity.

4.2 ROLE OF JOB SEPARATION RATE SHOCKS Our model includes a stochastic process for job separation rate shocks based on their careful measurement from the underlying employment flows data. Given this, we ask what role job separation rate shocks play in driving and propagating the business cycle. We begin by establishing that variation in the job separation rate is responsible for a significant fraction of business cycle variation in the economy. To show this, the top panel in Figure 1 reports the normalized forecast error variance decomposition for output, the job finding rate, unemployment, and vacancies in the linear model. In each plot, we decompose the volatility into three components attributable to variation in the job separation rate, labor productivity, and their interaction. The forecast error variance is normalized by the sum of these three components, since the correlation between the shocks implies that the contributions will not necessarily sum to unity.[11]

In all cases, variation in only the job separation rate accounts for at least 20% of the overall volatility. In particular, job separation rate shocks account for 60% of short-run unemployment volatility and close to 50% of the volatility at longer horizons. This result appears to contrast with the analysis in Shimer (2012), which concludes that separation rate variation accounts for no more than 25% of unemployment volatility. We emphasize that our model is consistent with this reduced-form result (see the last row of Table 4) but are able to go a step further by decomposing unemployment into its structural components. Importantly, our decomposition shows that job separation rate shocks account for about 30% of the variation in the job finding rate. Once we account for this, the contribution of separation rate shocks to unemployment volatility naturally increases.

We compute the same decomposition in the nonlinear model, as shown in the bottom panel of Figure 1.[12] In this case, the contribution of separation rate shocks to unemployment variation declines but remains substantial at 40%. The fall relative to the linear model is primarily driven by the stronger contribution of the shock correlation (25% in the nonlinear model vs. 14% in the linear model). Intuitively, the nonlinear model endogenously generates feedback between the two shocks in addition to their exogenous correlation. Furthermore, this contribution of separation rate shocks to unemployment volatility is consistent with Barnichon (2012) who estimates a reduced-form decomposition that controls for the dependence of the job finding rate on the separation rate.

Impulse Responses The left column of Figure 2 plots the impulse responses to two types of job separation rate shocks in the linear and nonlinear model. Once again, we begin by discussing the results from the linear model. Under the "interacted" shock, labor productivity responds according to the estimated correlation coefficient ρ_{as}. With the "pure" shock, the correlation between labor productivity and job separations is turned off so only the separation rate responds to the shock.[13] In both cases, the shock implies the separation rate increases by two standard deviations on impact.

[11] Isakin and Ngo (2020) use the same approach to normalize the forecast error variance for a fully nonlinear model.

[12] The nonlinear decomposition follows Lanne and Nyberg (2016). Appendix D describes our implementation.

[13] The "pure shock" solves for $\{\varepsilon_{s,t+1}, \varepsilon_{a,t+1}\}$ so $\rho_{as}\sigma_a\varepsilon_{a,t+1} + \sigma_s\varepsilon_{s,t+1} = 2\sigma_s$ and $\rho_{as}\sigma_s\varepsilon_{s,t+1} + \sigma_a\varepsilon_{a,t+1} = 0$.

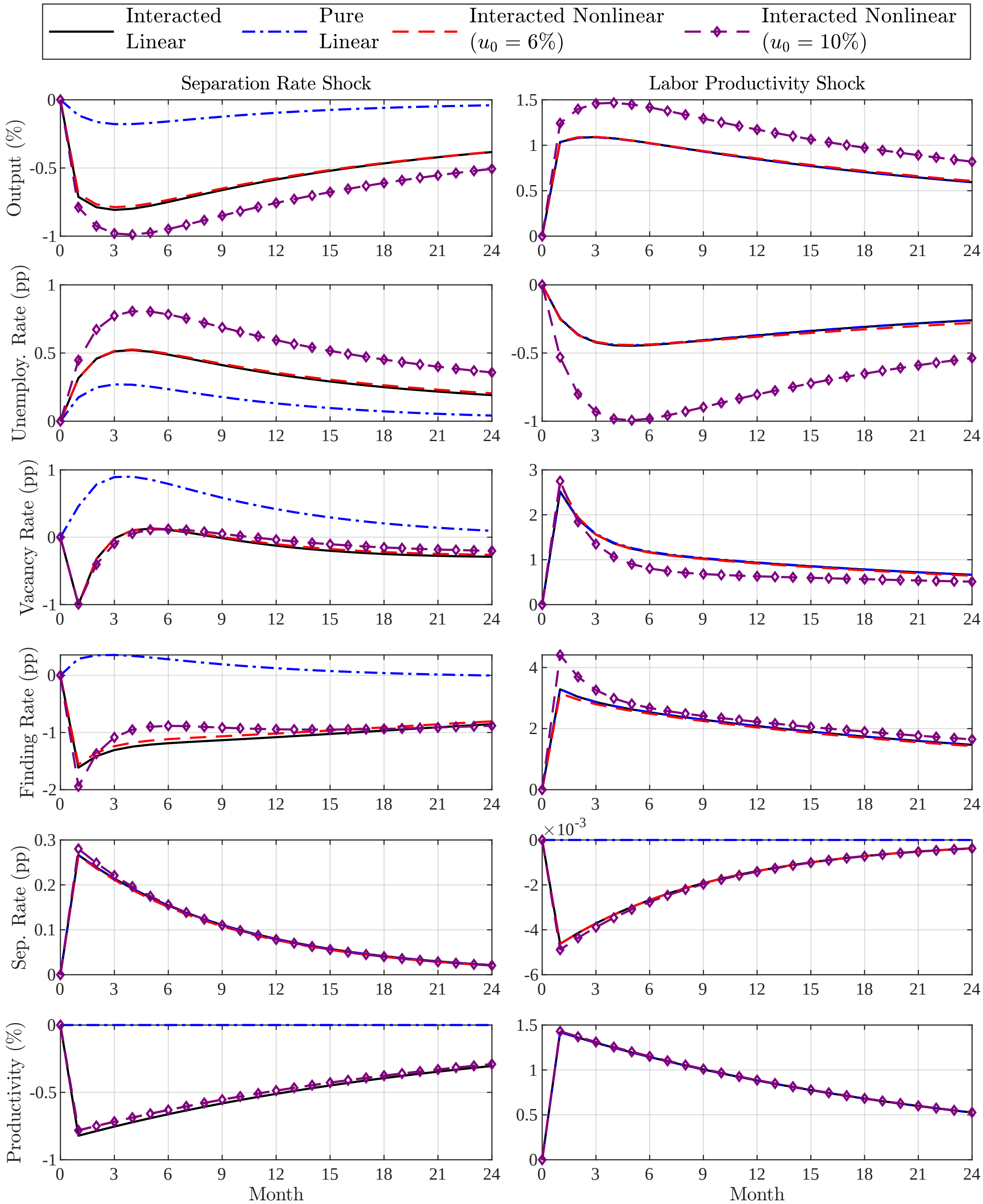

Figure 2: Impulse responses to a +2SD shock in percent (%) or percentage point (pp) deviations from steady state. The "Pure Shock" only affects the exogenous variable being shocked, while the "Interacted Shock" includes the cross-effect caused by the correlation between the job separation rate and labor productivity.

Consider first the more empirically relevant case of the "interacted shock". In response to a 0.3 percentage point increase in the separation rate and the associated 0.8% decrease in labor productivity, macroeconomic activity declines. Output falls by 0.8% and the unemployment rate increases by 0.5 percentage points. The response of vacancies reflects two opposing forces. First, the decline in labor productivity lowers the profitability of new hires and causes a drop in vacancy creation. Second, the increase in unemployment raises the job filling rate, lowering the marginal cost of vacancy creation. The drop in marginal costs causes vacancies to quickly rebound before declining again. As a result of the increase in unemployment and decline in vacancy creation, the job finding rate drops by 1.6 percentage points in response to the positive separation rate shock.

When we artificially shut down the correlation between job separations and labor productivity, the macroeconomic responses are qualitatively different. Without the decline in labor productivity, vacancy creation increases in response to the shock since the job filling rate is higher. As a result, the job finding rate slightly increases on impact. Together, these responses mute the increase in unemployment and decline in output stemming from the shock. These results highlight the importance of accounting for the correlation between the job separation rate and labor productivity when analyzing the transmission of separation rate shocks.[14] While pure separation rate shocks produce counterfactual positive co-movements between unemployment and vacancies (Shimer, 2005), allowing for a realistic degree of correlation with labor productivity corrects this behavior (Table 5 shows the unconditional correlation of unemployment and vacancies is close to the data).

To quantitatively assess the degree of state-dependence, Figure 2 compares the impulse responses from the linear model to generalized impulse responses from the nonlinear model, computed according to Koop et al. (1996). As expected, when the economy is initialized in steady state ($u_0 = 6\%$), the nonlinear responses are nearly identical to the linear responses. However, the economy becomes more sensitive to shocks in a recession where the initial unemployment rate is 10%. An increase in either the job separation rate or labor productivity leads to larger responses of unemployment and hence output. The larger responses are due to a downward rigidity of marginal costs discussed in the context of productivity shocks by Petrosky-Nadeau et al. (2018). Figure 2 shows how this mechanism also applies to job separation rate shocks. When unemployment is high, the marginal cost of vacancy creation is depressed due to a high job filling rate. In response to a positive separation rate shock and the associated decline in labor productivity, the marginal cost runs into a downward rigidity since a drop in vacancies has only a minor effect on the job filling rate. Hence job creation falls more than in normal times, leading to a larger decline in the job finding rate. With more people out of work, unemployment rises and output declines more.

[14]Den Haan et al. (2000) provide a mechanism in which labor productivity shocks drive endogenous movements in the job separation rate. Our analysis suggests that mechanisms with the opposite direction of causality are also relevant. While we are deliberately agnostic about the sources of this correlation, our results suggest that future work could focus on developing micro-foundations for mechanisms that link labor productivity to changes in the rate of job separation.

4.3 ENDOGENOUS UNCERTAINTY The state-dependence in the nonlinear impulse responses is evidence that shocks to the first moments of exogenous variables induce changes in higher order moments of endogenous variables. For example, the conditional distribution of future output growth will depend on the state of the economy and the conditional distribution of exogenous shocks. This dependence generates endogenous uncertainty about the distribution of future output growth and allows us to relate our theoretical model to a burgeoning empirical literature that estimates the endogenous response of macroeconomic uncertainty to exogenous first moment shocks.

To connect to recent empirical work (Jurado et al., 2015; Ludvigson et al., 2020), we define uncertainty as the expected volatility of the h-month ahead forecast error for output growth given by

$$\mathcal{U}_{t,t+h}^{\Delta \log y} = \sqrt{E_t[(\Delta \log y_{t+h} - E_t[\Delta \log y_{t+h}])^2]}.$$

We will refer to structural fluctuations in this statistic as time-varying endogenous uncertainty.

We measure uncertainty in the data as the quarterly average of the monthly real uncertainty series ($h = 1$) from Ludvigson et al. (2020). This series is a sub-index of the macro uncertainty series from Jurado et al. (2015) that accounts for 73 real activity variables such as measures of output, income, housing, consumption, and inventories. To construct the uncertainty series, most variables are transformed into growth rates and standard normalized. Repeated simulations of a factor augmented vector autoregression are used to obtain estimates of uncertainty for each real variable and then averaged to generate the aggregate real uncertainty series. The benefit of this series is that it distinguishes between uncertainty and *ex-post* volatility. To make the units from our model directly comparable to the real uncertainty series, we calculate $SD(\mathcal{U}_{t,t+1}^{\Delta \log y})/SD(\Delta \log y_t)$.

Moment	Data	Nonlinear Model	Moment	Data	Nonlinear Model
$SD(\Delta \log y)$	0.86	1.03	$SD(\mathcal{U}_{t,t+1}^{\Delta \log y})$	5.68	4.85
$Corr(\Delta \log y, \mathcal{U}_{t,t+1}^{\Delta \log y})$	−0.37	−0.13	$AC(\mathcal{U}_{t,t+1}^{\Delta \log y})$	0.84	0.97

Table 6: Non-targeted uncertainty moments. The moments in the data are computed from the quarterly average of the monthly real uncertainty series ($h = 1$) from Ludvigson et al. (2020). The model-implied moments are based on the linear parameter estimates when both the goods and labor moments are targeted.

Table 6 compares uncertainty moments in the data to simulations of the nonlinear model given the mean parameter estimates from the linear model. The nonlinear model makes two noteworthy predictions. First, the model predicts that output growth uncertainty is counter-cyclical, consistent with the real uncertainty series in the data. Second, the volatility of output growth uncertainty is close to its empirical counterpart. This result indicates that the degree of state-dependence shown in Figure 2 is sufficient to endogenously generate most of the time-varying uncertainty in the data. It is also consistent with Ludvigson et al. (2020), who show empirically that uncertainty about real activity is often an endogenous response to business cycles rather than an exogenous propagation.

Finally, we decompose the response of output growth uncertainty into its structural components using the same decomposition applied in Figure 1b. We find job separation rate shocks alone account for 37% of the volatility in output growth uncertainty. This demonstrates that exogenous variation in the inflows to unemployment also have significant higher-order effects on the economy.

5 CONCLUSION

This paper shows an estimated real business cycle model with equilibrium unemployment is able to replicate a wide range of empirical business cycle moments. Our identification strategy highlights a new role for the elasticity of matches with respect to unemployment in generating realistic labor market volatility in unemployment and vacancies. We use our model to emphasize the importance of job separation rate shocks in driving unemployment volatility and also show that accounting for their correlation with labor productivity is crucial to produce a realistic transmission mechanism. Finally, we document that there is rich state-dependence in the responses to separation rate shocks, which endogenously generates empirically consistent fluctuations in output growth uncertainty.

There are several directions one could extend our benchmark model. First, we have abstracted from two margins that seem important for a complete account of business cycle labor market dynamics: on the job search and labor force participation. Second, we have intentionally built our insights on the foundation of existing representative household real business cycle models, and as such have abstracted from household heterogeneity in income, consumption, and wealth. Third, we have abstracted from nominal frictions, which would provide a role for monetary policy. Introducing these features into our quantitative framework could be useful goals for future research.

REFERENCES

ANDOLFATTO, D. (1996): "Business Cycles and Labor-Market Search," *American Economic Review*, 86, 112–132.

ARELLANO, C., Y. BAI, AND P. J. KEHOE (2019): "Financial Frictions and Fluctuations in Volatility," *Journal of Political Economy*, 127, 2049–2103, https://doi.org/10.1086/701792.

BARNICHON, R. (2010): "Building a composite Help-Wanted Index," *Economics Letters*, 109, 175–178, https://doi.org/10.1016/j.econlet.2010.08.029.

——— (2012): "Vacancy posting, job separation and unemployment fluctuations," *Journal of Economic Dynamics and Control*, 36, 315–330, https://doi.org/10.1016/j.jedc.2011.09.00.

BLANCHARD, O. AND J. GALÍ (2010): "Labor Markets and Monetary Policy: A New Keynesian Model with Unemployment," *American Economic Journal: Macroeconomics*, 2, 1–30, https://doi.org/10.1257/mac.2.2.1.

BRUNNERMEIER, M. K. AND Y. SANNIKOV (2014): "A Macroeconomic Model with a Financial Sector," *American Economic Review*, 104, 379–421, https://doi.org/10.1257/aer.104.2.379.

CHODOROW-REICH, G. AND L. KARABARBOUNIS (2016): "The Cyclicality of the Opportunity Cost of Employment," *Journal of Political Economy*, 124, 1563–1618, https://doi.org/10.1086/688876.

CHRISTIANO, L. J., M. S. EICHENBAUM, AND M. TRABANDT (2016): "Unemployment and Business Cycles," *Econometrica*, 84, 1523–1569, https://doi.org/10.3982/ECTA11776.

COLEMAN, II, W. J. (1991): "Equilibrium in a Production Economy with an Income Tax," *Econometrica*, 59, 1091–1104, https://doi.org/10.2307/2938175.

COLES, M. G. AND A. M. KELISHOMI (2018): "Do Job Destruction Shocks Matter in the Theory of Unemployment?" *American Economic Journal: Macroeconomics*, 10, 118–136, https://doi.org/10.1257/mac.20150040.

COSTAIN, J. S. AND M. REITER (2008): "Business cycles, unemployment insurance, and the calibration of matching models," *Journal of Economic Dynamics and Control*, 32, 1120–1155, https://doi.org/10.1016/j.jedc.2007.04.008.

DEN HAAN, W. J., G. RAMEY, AND J. WATSON (2000): "Job Destruction and Propagation of Shocks," *American Economic Review*, 90, 482–498, https://doi.org/10.1257/aer.90.3.482.

ELSBY, M. W. L., G. SOLON, AND R. MICHAELS (2009): "The Ins and Outs of Cyclical Unemployment," *American Economic Journal: Macroeconomics*, 1, 84–110, https://doi.org/10.1257/mac.1.1.84.

FAJGELBAUM, P., M. TASCHEREAU-DUMOUCHEL, AND E. SCHAAL (2017): "Uncertainty Traps," *The Quarterly Journal of Economics*, 132, 1641–1692, https://doi.org/10.1093/qje/qjx02.

FUJITA, S. AND G. RAMEY (2012): "Exogenous versus Endogenous Separation," *American Economic Journal: Macroeconomics*, 4, 68–93, https://doi.org/10.1257/mac.4.4.68.

GALINDEV, R. AND D. LKHAGVASUREN (2010): "Discretization of highly persistent correlated AR(1) shocks," *Journal of Economic Dynamics and Control*, 34, 1260–1276, https://doi.org/10.1016/j.jedc.2010.02.006.

GARCIA, C. B. AND W. I. ZANGWILL (1981): *Pathways to Solutions, Fixed Points and Equilibria*, Prentice-Hall series in computational mathematics, Prentice-Hall.

HAGEDORN, M. AND I. MANOVSKII (2008): "The Cyclical Behavior of Equilibrium Unemployment and Vacancies Revisited," *American Economic Review*, 98, 1692–1706, https://doi.org/10.1257/aer.98.4.1692.

HALL, R. E. (2005): "Employment Fluctuations with Equilibrium Wage Stickiness," *American Economic Review*, 95, 50–65, https://doi.org/10.1257/0002828053828482.

HALL, R. E. AND P. R. MILGROM (2008): "The Limited Influence of Unemployment on the Wage Bargain," *American Economic Review*, 98, 1653–1674, https://doi.org/10.1257/aer.98.4.1653.

HAMILTON, J. D. (2018): "Why You Should Never Use the Hodrick-Prescott Filter," *Review of Economics and Statistics*, 100, 831–843, https://doi.org/10.1162/rest_a_00706.

HODRICK, R. J. (2020): "An Exploration of Trend-Cycle Decomposition Methodologies in Simulated Data," NBER Working Paper 26750, https://doi.org/10.3386/w26750.

HODRICK, R. J. AND E. C. PRESCOTT (1997): "Postwar U.S. Business Cycles: An Empirical Investigation," *Journal of Money, Credit and Banking*, 29, 1–16, https://doi.org/10.2307/2953682.

ISAKIN, M. AND P. V. NGO (2020): "Variance Decomposition Analysis for Nonlinear Economic Models," *Oxford Bulletin of Economics and Statistics*, forthcoming.

JURADO, K., S. C. LUDVIGSON, AND S. NG (2015): "Measuring Uncertainty," *American Economic Review*, 105, 1177–1216, https://www.doi.org/10.1257/aer.20131193.

KOOP, G., M. H. PESARAN, AND S. M. POTTER (1996): "Impulse Response Analysis in Nonlinear Multivariate Models," *Journal of Econometrics*, 74, 119–147, https://doi.org/10.1016/0304-4076(95)01753-4.

KOPECKY, K. AND R. SUEN (2010): "Finite State Markov-chain Approximations to Highly Persistent Processes," *Review of Economic Dynamics*, 13, 701–714, https://doi.org/10.1016/j.red.2010.02.002.

LANNE, M. AND H. NYBERG (2016): "Generalized Forecast Error Variance Decomposition for Linear and Nonlinear Multivariate Models," *Oxford Bulletin of Economics and Statistics*, 78, 595–603, https://doi.org/10.1111/obes.12125.

LJUNGQVIST, L. AND T. J. SARGENT (2017): "The Fundamental Surplus," *American Economic Review*, 107, 2630–2665, https://doi.org/10.1257/aer.20150233.

LUDVIGSON, S. C., S. MA, AND S. NG (2020): "Uncertainty and Business Cycles: Exogenous Impulse or Endogenous Response?" *American Economic Journal: Marcoeconomics*, forthcoming.

MENDOZA, E. G. (2010): "Sudden Stops, Financial Crises, and Leverage," *American Economic Review*, 100, 1941–1966, https://doi.org/10.1257/aer.100.5.1941.

MERZ, M. (1995): "Search in the labor market and the real business cycle," *Journal of Monetary Economics*, 36, 269–300, https://doi.org/10.1016/0304-3932(95)01216-8.

MORTENSEN, D. AND E. NAGYPAL (2007): "More on Unemployment and Vacancy Fluctuations," *Review of Economic Dynamics*, 10, 327–347, https://doi.org/10.1016/j.red.2007.01.004.

NEWEY, W. K. AND K. D. WEST (1987): "A simple, positive semi-definite, heteroskedasticity and autocorrelation consistent covariance matrix," *Econometrica*, 55, 703–708, https://www.doi.org/10.2307/1913610.

PETRONGOLO, B. AND C. A. PISSARIDES (2001): "Looking into the Black Box: A Survey of the Matching Function," *Journal of Economic Literature*, 39, 390–431, https://doi.org/10.1257/jel.39.2.390.

PETROSKY-NADEAU, N. AND L. ZHANG (2017): "Solving the Diamond-Mortensen-Pissarides model accurately," *Quantitative Economics*, 8, 611–650, https://doi.org/10.3982/QE452.

PETROSKY-NADEAU, N., L. ZHANG, AND L.-A. KUEHN (2018): "Endogenous Disasters," *American Economic Review*, 108, 2212–2245, https://doi.org/10.1257/aer.20130025.

PISSARIDES, C. A. (2009): "The Unemployment Volatility Puzzle: Is Wage Stickiness the Answer?" *Econometrica*, 77, 1339–1369, https://doi.org/10.3982/ECTA7562.

PLANTE, M., A. W. RICHTER, AND N. A. THROCKMORTON (2018): "The Zero Lower Bound and Endogenous Uncertainty," *Economic Journal*, 128, 1730–1757, https://doi.org/10.1111/ecoj.12445.

RICHTER, A. W., N. A. THROCKMORTON, AND T. B. WALKER (2014): "Accuracy, Speed and Robustness of Policy Function Iteration," *Computational Economics*, 44, 445–476, https://doi.org/10.1007/s10614-013-9399-2.

ROUWENHORST, K. G. (1995): "Asset Pricing Implications of Equilibrium Business Cycle Models," in *Frontiers of Business Cycle Research*, ed. by T. F. Cooley, Princeton, NJ: Princeton University Press, 294–330.

RUGE-MURCIA, F. (2012): "Estimating nonlinear DSGE models by the simulated method of moments: With an application to business cycles," *Journal of Economic Dynamics and Control*, 36, 914–938, http:https://doi.org/10.1016/j.jedc.2012.01.00.

SHIMER, R. (2005): "The Cyclical Behavior of Equilibrium Unemployment and Vacancies," *American Economic Review*, 95, 25–49, https://doi.org/10.1257/0002828053828572.

——— (2012): "Reassessing the Ins and Outs of Unemployment," *Review of Economic Dynamics*, 15, 127–148, https://doi.org/10.1016/j.red.2012.02.001.

SIMS, C. A. (2002): "Solving Linear Rational Expectations Models," *Computational Economics*, 20, 1–20, https://doi.org/10.1023/A:1020517101123.

STRAUB, L. AND R. ULBRICHT (2015): "Endogenous Uncertainty and Credit Crunches," Toulouse School of Economics Working Paper 15-604.

VAN NIEUWERBURGH, S. AND L. VELDKAMP (2006): "Learning Asymmetries in Real Business Cycles," *Journal of Monetary Economics*, 53, 753–772, https://doi.org/10.1016/j.jmoneco.2005.02.003.

A DATA SOURCES AND TRANSFORMATIONS

We use the following time-series from 1955-2019 provided by Haver Analytics:

1. **Civilian Noninstitutional Population: 16 Years & Over**
   Not Seasonally Adjusted, Quarterly, Thousands (LN16N@USECON)

2. **Gross Domestic Product: Implicit Price Deflator**
   Seasonally Adjusted, Quarterly, 2012=100 (DGDP@USNA)
3. **Gross Domestic Product**
   Seasonally Adjusted, Quarterly, Billions of Dollars (GDP@USECON)
4. **Personal Consumption Expenditures: Nondurable Goods**
   Seasonally Adjusted, Quarterly, Billions of Dollars (CN@USECON)
5. **Personal Consumption Expenditures: Services**
   Seasonally Adjusted, Quarterly, Billions of Dollars (CS@USECON)
6. **Private Fixed Investment**
   Seasonally Adjusted, Quarterly, Billions of Dollars (F@USECON)
7. **Personal Consumption Expenditures: Durable Goods**
   Seasonally Adjusted, Quarterly, Billions of Dollars (CD@USECON)
8. **Output Per Person**, Non-farm Business Sector, All Persons,
   Seasonally Adjusted, Quarterly, 2012=100 (LXNFS@USNA)
9. **Labor Share**, Non-farm Business Sector, All Persons,
   Seasonally Adjusted, Quarterly, Percent (LXNFBL@USNA)
10. **Compensation**, Non-farm Business Sector, All Persons,
    Seasonally Adjusted, Quarterly, 2012=100 (LXNFF@USNA)
11. **Employment**, Non-farm Business Sector, All Persons,
    Seasonally Adjusted, Quarterly, 2012=100 (LXNFM@USNA)
12. **Unemployed, 16 Years & Over**
    Seasonally Adjusted, Monthly, Thousands (LTU@USECON)
13. **Civilian Unemployment Rate: 16 yr & Over**
    Seasonally Adjusted, Monthly, Percent (LR@USECON)
14. **Civilian Labor Force: 16 yr & Over**
    Seasonally Adjusted, Monthly, Thousands (LF@USECON)
15. **Civilians Unemployed for Less Than 5 Weeks**
    Seasonally Adjusted, Monthly, Thousands (LU0@USECON)
16. **Net Stock: Private Fixed Assets**, Billions of Dollars (EPT@CAPSTOCK)
17. **Net Stock: Consumer Durable Goods**, Billions of Dollars (EDT@CAPSTOCK)
18. **Depreciation: Private Fixed Assets**, Billions of Dollars (KPT@CAPSTOCK)
19. **Depreciation: Consumer Durable Goods**, Billions of Dollars (KDT@CAPSTOCK)

We also use the Help Wanted Advertising Index (HWI) from Barnichon (2010), which is in units of the labor force. This series corrects for online advertising and is available on the author's website. We applied the following transformations to the above data sources:

1. **Per Capita Real Output Growth**:

$$\Delta \log Y_t = 100 \left(\log \left(\tfrac{GDP_t}{DGDP_t + LN16N_t} \right) - \log \left(\tfrac{GDP_{t-1}}{DGDP_{t-1} + LN16N_{t-1}} \right) \right).$$

2. **Per Capita Real Consumption Growth**:

$$\Delta \log C_t = 100 \left(\log \left(\tfrac{CN_t + CS_t}{DGDP_t + LN16N_t} \right) - \log \left(\tfrac{CN_{t-1} + CS_{t-1}}{DGDP_{t-1} + LN16N_{t-1}} \right) \right).$$

3. **Per Capita Real Investment Growth**:

$$\Delta \log I_t = 100 \left(\log \left(\tfrac{F_t + CD_t}{DGDP_t + LN16N_t} \right) - \log \left(\tfrac{F_{t-1} + CD_{t-1}}{DGDP_{t-1} + LN16N_{t-1}} \right) \right).$$

4. **Vacancy Rate**: HWI from 1954M1-2000M12 and $LJJTLA/LF$ from 2001M1-2019M12.
5. **Short-term Unemployed** (U^s): The redesign of the Current Population Survey (CPS) in 1994 reduced u_t^s. To correct for this bias, we use IMPUMS-CPS data to scale u_t^s by the ratio of u_t^s/u_t for the first and fifth rotations groups to u_t^s/u_t across all rotation groups. In addition to the 9 mandatory identification variables, we first extract the following: EMPSTAT ("Employment Status"), DURUNEMP ("Continuous weeks unemployed") and MISH ("Month in sample, household level"). Unemployed persons have EMPSTAT of 20, 21, or 22. Short-term unemployed are persons who are unemployed and DURUNEMP is 5 or less. Incoming rotation groups have MISH of 1 or 5. Using the final weights, WTFINL, we then calculate unemployment rates conditional on the appropriate values of MISH and DURUNEMP. We then apply the X-12 seasonal adjustment function in STATA to the time series for the ratio. Finally, we take an average of the seasonally adjusted time series. This process yields an average ratio of 1.1693, so U^s equals $LU0$ before 1994 and $1.1693 \times LU0$ after 1994.
6. **Job-Finding Rate**: $f_t = 1 - (LTU_t - U_t^s)/LTU_{t-1}$.
7. **Separation Rate**: $s_t = 1 - \exp(-\tilde{s}_t)$, where $\tilde{s}_t$ satisfies

$$LTU_{t+1} = \frac{(1 - \exp(-\tilde{f}_t - \tilde{s}_t))\tilde{s}_t LF_t}{\tilde{f}_t + \tilde{s}_t} + \exp(-\tilde{f}_t - \tilde{s}_t) LTU_t,$$

   and $\tilde{f}_t = -\log(1 - f_t)$.
8. **Net Unemployment Inflow Rate**: $z_t = U_t^s/(LF_{t-1} - LTU_{t-1})$.
9. **Real Wage**: $w_t = 100 \times LXNFF_t/(LXNFM_t \times DGDP_t)$

10. **Capital Depreciation Rate**:

$$\delta = (KPT + KDT)/(EPT + EDT).$$

All monthly time series are averaged to a quarterly frequency. The data is detrended using a Hamilton filter with an 8 quarter window. All empirical targets are computed using quarterly data.

B ESTIMATION METHOD

The estimation procedure has two stages. The first stage estimates moments in the data using a 2-step Generalized Method of Moments (GMM) estimator with a Newey and West (1987) weighting matrix with 5 lags. The second stage is a Simulated Method of Moments (SMM) procedure that searches for a parameter vector that minimizes the distance between the mean GMM estimates in the data and short-sample predictions of the model, weighted by the diagonal of the GMM estimate of the variance-covariance matrix. The second stage is repeated for many different draws of shocks to obtain a sampling distribution for each parameter. The following steps outline the algorithm:

1. Use GMM to estimate the moments, $\hat{\Psi}_T^D$, and the diagonal of the covariance matrix, $\hat{\Sigma}_T^D$.
2. Use SMM to estimate the linear structural model. Given a random seed, h, draw a $B + 3T$ period sequence for each shock in the model, where B is a $1{,}000$ period burn-in and $3T$ is the sample size of the monthly time series. Denote the shock matrix by $\mathcal{E}^h = [\varepsilon_s^h, \varepsilon_a^h]_{t=1}^{B+3T}$).

   For shock sequence $h \in \{1, \dots, N_h\}$, run the following steps:

   (a) Specify a guess, $\hat{\theta}_0$, for the N_p estimated parameters and the covariance matrix, $\Sigma_P^{h,0}$. For all $i \in \{1, \dots, N_m\}$, apply the following steps:

      i. Draw $\hat{\theta}_i$ from a multivariate normal distribution centered at some mean parameter vector, $\bar{\theta}$, with a diagonal covariance matrix, Σ_0.

      ii. Solve the linear model with Sims's (2002) `gensys` algorithm given $\hat{\theta}_i$. Repeat the previous step if the solution does not exist or is not unique.

      iii. Given $\mathcal{E}^h(r)$, simulate the monthly model R times for $B + 3T$ periods. We draw initial states from the ergodic distribution by burning off the first B periods. Aggregate variables in levels by summing and aggregate rates by averaging to a quarterly frequency. For each repetition r, calculate the moments based on T quarters, $\Psi_T^M(\hat{\theta}_i, \mathcal{E}^h(r))$, the same length as the quarterly data.

      iv. Calculate the median moments across the R simulations,

$$\bar{\Psi}_{R,T}^M(\hat{\theta}_i, \mathcal{E}^h) = \text{median}\{\Psi_T^M(\hat{\theta}_i, \mathcal{E}^h(r))\}_{r=1}^R,$$

and evaluate the loss function:,

$$J_i^h = [\hat{\Psi}_T^D - \bar{\Psi}_{R,T}^M(\hat{\theta}_i, \mathcal{E}^h)]'[\hat{\Sigma}_T^D(1+1/R)]^{-1}[\hat{\Psi}_T^D - \bar{\Psi}_{R,T}^M(\hat{\theta}_i, \mathcal{E}^h)].$$

(b) Find the parameter draw $\hat{\theta}_0$ that corresponds to $\min\{J_i^h\}_{i=1}^{N_d}$, and calculate $\Sigma_P^{h,0}$.

  i. Find the N_{best} draws with the lowest J_i^h. Stack the remaining draws in a $N_{best} \times N_p$ matrix, $\hat{\Theta}^h$, and define $\tilde{\Theta}^h = \hat{\Theta}^h - \mathbf{1}_{N_{best}\times 1} \sum_{i=N_{best}}^{N_d} \hat{\theta}_i^h/(N_{best})$.

  ii. Calculate $\Sigma_{P,0} = (\tilde{\Theta}^h)'\tilde{\Theta}^h/(N_{best})$.

(c) Minimize J with simulated annealing. For $i \in \{0, \ldots, N_d\}$, repeat the following steps:

  i. Draw a candidate vector of parameters, $\hat{\theta}_i^{cand}$, where

$$\hat{\theta}_i^{cand} \sim \begin{cases} \hat{\theta}_0 & \text{for } i = 0, \\ \mathbb{N}(\hat{\theta}_{i-1}, c_0\Sigma_P^{h,0}) & \text{for } i > 0. \end{cases}$$

  We set c_0 to target an average acceptance rate of 50% across seeds.

  ii. Under Step 2a, repeats Steps ii-iv.

  iii. Accept or reject the candidate draw according to

$$(\hat{\theta}_i^h, J_i^h) = \begin{cases} (\hat{\theta}_i^{cand}, J_i^{h,cand}) & \text{if } i = 0, \\ (\hat{\theta}_i^{cand}, J_i^{h,cand}) & \text{if } \min(1, \exp(J_{i-1}^h - J_i^{h,cand})/c_1) > \hat{u}, \\ (\hat{\theta}_{i-1}, J_{i-1}^h) & \text{otherwise,} \end{cases}$$

  where c_1 is the temperature and $\hat{u}$ is a draw from a uniform distribution.

(d) Find the parameter draw $\hat{\theta}_{\min}^h$ that corresponds to $\min\{J_i^h\}_{i=1}^{N_d}$, and update Σ_P^h.

  i. Discard the first $N_d/2$ draws. Stack the remaining draws in a $N_d/2 \times N_p$ matrix, $\hat{\Theta}^h$, and define $\tilde{\Theta}^h = \hat{\Theta}^h - \mathbf{1}_{N_d/2\times 1} \sum_{i=N_d/2}^{N_d} \hat{\theta}_i^h/(N_d/2)$.

  ii. Calculate $\Sigma_P^{h,up} = (\tilde{\Theta}^h)'\tilde{\Theta}^h/(N_d/2)$.

(e) Repeat the previous step N_{SMM} times, initializing at draw $\hat{\theta}_0 = \hat{\theta}_{\min}^h$ and covariance matrix $\Sigma_P = \Sigma_P^{h,up}$. Gradually decrease the temperature. Of all the draws, find the lowest J value, denoted J_{guess}^h, and the corresponding draws, θ_{guess}^h.

(f) Minimize the same loss function with MATLAB's `fminsearch` starting at θ_{guess}^h. The resulting minimum is $\hat{\theta}_{\min}^h$ with a loss function value of $J_{\min}^h$. Repeat, each time updating the guess, until $J_{guess}^h - J_{\min}^h < 0.001$. The parameter estimates reported in Table 3 of the main paper, denoted $\hat{\theta}^h$, correspond to the final $J_{\min}^h$.

The set of SMM parameter estimates $\{\hat{\theta}^h\}_{h=1}^{N_h}$ approximate the joint sampling distribution of the parameters. We report its mean, $\bar{\theta} = \sum_{h=1}^{N_h} \hat{\theta}^h/N_h$, and $(5, 95)$ percentiles. For the targeted and non-targeted moments, we report the mean, $\bar{\Psi}_T^M = \sum_{h=1}^{N_h} \bar{\Psi}_{R,T}^M(\hat{\theta}^h, \mathcal{E}^h)/N_h$, and the corresponding t-statistic for moment m, $(\bar{\Psi}_T^M(m) - \hat{\Psi}_T^D(m))/(\hat{\Sigma}_T^D(m,m))^{1/2}$.

We set $N_h = 100$, $R = 1{,}001$, and $N_{SMM} = 5$. N_m, N_d, N_p, and c_1 are all model-specific. The SMM algorithm is programmed in Fortran 95 with Open MPI and executed on the BigTex cluster.

C SOLUTION METHODS

Nonlinear Solution The nonlinear equilibrium system can be compactly written as

$$E_t[g(\mathbf{x}_{t+1}, \mathbf{x}_t, \varepsilon_{t+1})|\mathbf{z}_t, \vartheta] = 0,$$

where g is a vector-valued function, $\mathbf{x}_t$ is a vector of variables, $\varepsilon_t = \{s_t, a_t\}$ is a vector of shocks, $\mathbf{z}_t$ is a vector of endogenous and exogenous state variables, and ϑ is a vector of model parameters.

To approximate s_t and a_t we use the Markov chain in Rouwenhorst (1995), which Kopecky and Suen (2010) show outperforms other methods for approximating highly-persistent processes. We generalize this method to allow for cross correlation between s_t and a_t following Galindev and Lkhagvasuren (2010). Specifically, we define $\ln s_t \equiv \ln r_{1,t}$ and $\ln a_t \equiv \ln r_{2,t} + \rho_3 \ln r_{3,t}$ such that

$$\begin{aligned} \ln r_{1,t} &= (1-\rho_s)\ln \bar{s} + \rho_s \ln r_{1,t-1} + \sigma_1 \varepsilon_{1,t}, \\ \ln r_{2,t} &= (1-\rho_a)\ln \bar{a} + \rho_a \ln r_{2,t-1} + \sigma_2 \varepsilon_{2,t}, \\ \ln r_{3,t} &= \rho_a \ln r_{3,t-1} + \sigma_1 \varepsilon_{1,t}. \end{aligned}$$

The new system satisfies the following moment restrictions:

$$\begin{aligned} Var(\ln s_t) &= \frac{(\rho_{as}\sigma_a)^2 + \sigma_s^2}{1-\rho_s^2} = Var(\ln r_{1,t}) = \frac{\sigma_1^2}{1-\rho_s^2}, \\ Cov(\ln s_t, \ln a_t) &= \frac{\rho_{as}(\sigma_s^2 + \sigma_a^2)}{1-\rho_s\rho_a} = Cov(\ln r_{1,t}, \ln r_{2,t} + \rho_3 r_{3,t}) = \frac{\rho_3\sigma_1^2}{1-\rho_s\rho_a}, \\ Var(\ln a_t) &= \frac{(\rho_{as}\sigma_s)^2 + \sigma_a^2}{1-\rho_a^2} = Var(\ln r_{2,t} + \rho_3 \ln r_{3,t}) = \frac{\sigma_2^2}{1-\rho_a^2} + \frac{(\rho_3\sigma_1)^2}{1-\rho_a^2}, \end{aligned}$$

which allows us to solve for the parameters of the new processes,

$$\sigma_1 = \sqrt{(\rho_{as}\sigma_a)^2 + \sigma_s^2}, \quad \rho_3 = \rho_{as}(\sigma_s^2 + \sigma_a^2)/\sigma_1^2, \quad \sigma_2 = \sqrt{(\rho_{as}\sigma_s)^2 + \sigma_a^2 - (\rho_3\sigma_1)^2}.$$

The transformed variables $\ln r_{1,t}$ and $\ln r_{2,t}$ are approximated with independent Markov chains, while $\ln r_{3,t}$ is centered at zero on the interval $[-3,3]SD(\ln r_3)$, where $SD(\ln r_3) = \sigma_1/\sqrt{1-\rho_a^2}$. The bounds on the endogenous states, n_{t-1} and k_{t-1}, are set to $[-12\%, +3\%]$ and $[-8\%, +5\%]$ of their deterministic steady-state values, $\bar{n}$ and $\bar{k}$, which contain at least 99% of the ergodic distribution. We discretize $r_{1,t}$, $r_{2,t}$, n_{t-1}, k_{t-1}, and $r_{3,t}$ into 11, 11, 15, 15, and 15 evenly-spaced points, respectively. The product of the points in each dimension, D, is the total nodes in the state space ($D = 408{,}375$). The realization of $\mathbf{z}_t$ on node d is denoted $\mathbf{z}_t(d)$. The Rouwenhorst method provides integration nodes, $[r_{1,t+1}(m), r_{2,t+1}(m)]$, with weights, $\phi(m)$, for $m \in \{1, \ldots, M\}$. Since they evolve according to Markov chains, the number of realizations of $r_{j,t+1}$ is the same as $r_{j,t}$ (11).

Since vacancies $v_t \geq 0$, we introduce an auxiliary variable, ζ_t, such that $v_t = \max\{0, \zeta_t\}^2$ and $\lambda_{0,t} = \max\{0, -\zeta_t\}^2$, where $\lambda_{0,t}$ is the Lagrange multiplier on the non-negativity constraint. If $\zeta_t \geq 0$, then $v_t = \zeta_t^2$ and $\lambda_{0,t} = 0$. When $\zeta_t < 0$, the constraint is binding, $v_t = 0$, and $\lambda_{0,t} = \zeta_t^2$. Therefore, the constraint on v_t is transformed into a pair of equalities (Garcia and Zangwill, 1981).

The vector of policy functions and the realization on node d are denoted $\mathbf{pf}_t$ and $\mathbf{pf}_t(d)$, where $\mathbf{pf}_t \equiv [\zeta_t(\mathbf{z}_t), c_t(\mathbf{z}_t)]$. The following steps outline our nonlinear policy function iteration algorithm:

1. Use Sims's (2002) `gensys` algorithm to solve the log-linear model. Then map the solution for the policy functions to the discretized state space. This provides an initial conjecture.
2. On iteration $j \in \{1, 2, \ldots\}$ and each node $d \in \{1, \ldots, D\}$, use Chris Sims's `csolve` to find $\mathbf{pf}_t(d)$ to satisfy $E[g(\cdot)|\mathbf{z}_t(d), \vartheta] \approx 0$. Guess $\mathbf{pf}_t(d) = \mathbf{pf}_{j-1}(d)$. Then apply the following:
   (a) Solve for all variables dated at time t, given $\mathbf{pf}_t(d)$ and $\mathbf{z}_t(d)$.
   (b) Linearly interpolate the policy functions, $\mathbf{pf}_{j-1}$, at the updated state variables, $\mathbf{z}_{t+1}(m)$, to obtain $\mathbf{pf}_{t+1}(m)$ on every integration node, $m \in \{1, \ldots, M\}$.
   (c) Given $\{\mathbf{pf}_{t+1}(m)\}_{m=1}^M$, solve for the other elements of $\mathbf{x}_{t+1}(m)$ and compute
   $$E[g(\mathbf{x}_{t+1}, \mathbf{x}_t(d), \varepsilon_{t+1})|\mathbf{z}_t(d), \vartheta] \approx \textstyle\sum_{m=1}^M \phi(m) g(\mathbf{x}_{t+1}(m), \mathbf{x}_t(d), \varepsilon_{t+1}(m)).$$

   When `csolve` converges, set $\mathbf{pf}_j(d) = \mathbf{pf}_t(d)$.
3. Repeat step 2 until $\text{maxdist}_j < 10^{-8}$, where $\text{maxdist}_j \equiv \max\{|\mathbf{pf}_j - \mathbf{pf}_{j-1}|\}$. When that criterion is satisfied, the algorithm has converged to an approximate nonlinear solution.

Linear Solution We solve the following equilibrium system by applying Sims (2002) method:

$$\hat{n}_t = (1 - \bar{s})\hat{n}_{t-1} + \bar{s}(\hat{q}_t + \hat{v}_t - \hat{s}_t)$$
$$\hat{\theta}_t = \hat{v}_t - \hat{u}_t^s$$
$$\bar{u}^s \hat{u}_t^s = \bar{u}\hat{u}_{t-1} + \chi\bar{s}\bar{n}(\hat{s}_t + \hat{n}_{t-1})$$
$$\bar{u}\hat{u}_t + \bar{n}\hat{n}_t = 0$$
$$\hat{y}_t = \alpha\hat{k}_{t-1} + (1 - \alpha)(\hat{a}_t + \hat{n}_t)$$
$$\bar{c}\hat{c}_t + \bar{\imath}\hat{\imath}_t + \kappa\bar{v}\hat{v}_t = \bar{y}\hat{y}_t$$
$$\hat{q}_t = -\bar{\theta}^\iota\hat{\theta}_t/(1 + \bar{\theta}^\iota)$$
$$\hat{f}_t = \hat{\theta}_t + \hat{q}_t$$

$$\bar{w}\hat{w}_t = \eta\bar{w}_f\hat{w}_{f,t} + \beta\eta\kappa(1-\chi\bar{s})\bar{\theta}(E_t\hat{x}_{t+1} + E_t\hat{\theta}_{t+1} - \tfrac{\chi\bar{s}}{1-\chi\bar{s}}E_t\hat{s}_{t+1})$$
$$-(\kappa/\bar{q})\hat{q}_t = \bar{w}_f\hat{w}_{f,t} - \bar{w}\hat{w}_t + \beta(1-\bar{s})(\kappa/\bar{q})(E_t\hat{x}_{t+1} - E_t\hat{q}_{t+1} - \tfrac{\bar{s}}{1-\bar{s}}E_t\hat{s}_{t+1})$$
$$\hat{x}_{t+1} = \hat{c}_t - \hat{c}_{t+1}$$
$$(1/\nu)(\hat{\imath}_t - \hat{k}_{t-1}) = E_t\hat{x}_{t+1} + \beta\bar{r}^k E_t\hat{r}^k_{t+1} + (\beta/\nu)(E_t\hat{\imath}_{t+1} - \hat{k}_t)$$
$$\hat{k}_t = (1-\delta)\hat{k}_{t-1} + \delta\hat{\imath}_t$$
$$\hat{r}^k_t = \hat{y}_t - \hat{k}_{t-1}$$
$$\hat{w}_{f,t} = \hat{y}_t - \hat{n}_t$$
$$\bar{z}\hat{z}_t = \bar{z}\hat{s}_t - \chi\bar{s}\bar{f}\hat{f}_t$$
$$\hat{\theta}_d = \hat{v}_t - \hat{u}_{t-1}$$
$$\hat{a}_t = \rho_a\hat{a}_{t-1} + \rho_{as}\sigma_s\varepsilon_{s,t+1} + \sigma_a\varepsilon_{a,t+1}$$
$$\hat{s}_t = \rho_s\hat{s}_{t-1} + \rho_{as}\sigma_a\varepsilon_{a,t+1} + \sigma_s\varepsilon_{s,t+1}$$

where hats denote log deviations from the deterministic steady state ($\hat{x}_t = \log x_t - \log\bar{x}$).

D GENERALIZED IMPULSE RESPONSES AND VARIANCE DECOMPOSITION

A linear impulse response function (IRF) can be generalized to a nonlinear model. The key differences from a linear IRF are that a generalized IRF (GIRF) might vary with the initial states (e.g., whether unemployment is low or high) or be a nonlinear function of the size of the shock of interest. Following Koop et al. (1996), the GIRF of variable x_{t+h} over horizon h is given by

$$\mathcal{G}^j_t(x_{t+h}|\varepsilon_{j,t+1} = \xi_j, \mathbf{z}_t) = E_t[x_{t+h}|\varepsilon_{j,t+1} = \xi_j, \mathbf{z}_t] - E_t[x_{t+h}|\mathbf{z}_t],$$

where ξ_j is the size of shock $j \in \{s, a\}$ and $\mathbf{z}_t$ is a vector of initial states. The conditional expectations are computed based on the mean path from 10,000 simulations of the nonlinear model.

Likewise, a linear forecast error variance decomposition (FEVD) can be generalized to a nonlinear model by replacing the linear IRF with the GIRF. Thus, the generalized FEVD (GFEVD) inherits the possible state dependency and nonlinearity of the GIRF. Following Lanne and Nyberg (2016), the GFEVD of variable x_{t+h} into component j over time horizon h is given by

$$\lambda^j_t(x_{t+h}|\mathbf{z}_t) = \int_{-\infty}^{\infty} \frac{\sum_{\ell=1}^{h}\left(\mathcal{G}(x_{t+\ell}|\varepsilon_{j,t+1} = \xi_j, \mathbf{z}_t)\right)^2}{\sum_{j=1}^{m}\sum_{\ell=1}^{h}\left(\mathcal{G}(x_{t+\ell}|\varepsilon_{j,t+1} = \xi_j, \mathbf{z}_t)\right)^2} f(\xi_j)d\xi_j,$$

where $f(\cdot)$ is the probability density function of ε_j. In nonlinear models, the magnitude of the response of an endogenous variable to an exogenous innovation is not necessarily a linear function of the shock size. Thus, we report the nonlinear model GFEVD after integrating across the shock using Gauss Hermite quadrature. We normalize the GFEVD the same way as the linear FEVD.